The Interaction of Polyphenols with Bilayers: Conditions for Increasing Bilayer Adhesion

Nam-Won Huh,* N. A. Porter,# T. J. McIntosh,§ and S. A. Simon*
*Departments of Neurobiology and §Cell Biology, Duke University Medical Center, Durham, North Carolina 27710, and #Department of Chemistry, Duke University, Durham, North Carolina 27706 USA

ABSTRACT Because proteins and other molecules with a high polyphenol content are commonly involved in adhesion processes, we are investigating the interactions between polyphenols and biological materials. A naturally occurring polyphenol that binds a variety of proteins and lipids is tannic acid (TA), which contains five digallic acid residues covalently linked to a central D-glucose. A previous study has shown that TA increases the adhesion between apposing phosphatidylcholine (PC) bilayers and over a very narrow concentration range collapses the interbilayer fluid space from about 15 Å to 5 Å. To determine the chemical requirements a polyphenolic molecule must possess to increase bilayer adhesion, we have synthesized several simpler TA analogs that vary in their size, shape, and number of gallic acid and hydroxyl groups. X-ray diffraction, absorbance, binding, and differential scanning calorimetry measurements were used to investigate the interaction of these polyphenolic molecules with egg PC (EPC) and dipalmitoyl PC (DPPC) bilayers. Of these synthetic polyphenols, only penta-O-galloyl-α-D-glucose (PGG) was able to completely mimic the effects of TA by collapsing the interbilayer fluid space from 15 Å to 5 Å, decreasing the dipole potential by about 300 mV, increasing the transition enthalpy of DPPC liposomes, and inducing an interdigitated phase in DPPC. Binding studies indicated that the fluid space was reduced to 5 Å at an EPC:PGG mole ratio of 5:1. We conclude that these polyphenols collapse the fluid space of PC bilayers because they 1) are amphipathic and partition into the bilayers interfacial region, 2) are long enough to span the interbilayer space, 3) contain several gallic acids distributed so that they can partition simultaneously into apposing bilayers, and 4) have sufficient gallic acid residues to interact with all lipid headgroups and cover the bilayer surface. Under these conditions we conclude that the polyphenols form interbilayer bridges. We argue that these bridges are stabilized by increased adhesion arising from an increased van der Waals interaction between apposing bilayers, electrostatic interactions between the π electrons in the phenol ring and the $-(N^+CH_3)_3$ groups on the PC headgroups, decreased hydration repulsion between bilayers, and hydrogen bonds between the H-bond-donating moieties on the polyphenols and H-bond-accepting groups in the bilayer.

INTRODUCTION

Adhesion between biological membranes occurs primarily through specific proteins that form molecular bridges that stabilize intermembrane interactions (Springer, 1990). Because such systems are inherently complex, relatively little is known about the intermembrane separations and adhesion energies involved in these interactions. In contrast, the nonspecific adhesion between lipid bilayers, such as phosphatidylcholines (PC), are now reasonably well understood (Evans, 1991). The magnitude of the adhesion energy is determined by the balance between nonspecific attractive and repulsive energies (Evans and Parsegian, 1986). For PCs the attractive interaction is thought to arise entirely from van der Waals interactions (Israelachvili, 1985; Parsegian et al., 1979), although for other neutral lipids, such as phosphatidylethanolamines, interbilayer H bonds through water bridges or direct electrostatic interactions between apposing headgroups also contribute to the attractive interactions (McIntosh and Simon, 1986a; Seddon et al., 1984; Rand et al., 1988; Damodaran and Merz, 1994; McIntosh and Simon, 1996). Even between hydrated neutral bilayers there are several repulsive interactions that have markedly different ranges and magnitudes that are not always easy to separate. These include a short-range hydration pressure, which arises from the reorientation of the water interacting with the bilayer surface (Marcelja and Radic, 1976; Le-Neveu et al., 1977; Parsegian et al., 1979; McIntosh and Simon, 1986b; Rand et al., 1988; Rand and Parsegian, 1989; McIntosh and Simon, 1993), and steric pressures that depend on the size and volume fraction of the headgroups (McIntosh et al., 1987, 1989a; McIntosh and Simon, 1994b), thermally induced out-of-plane undulations of the bilayer (Helfrich, 1973; Helfrich and Servuss, 1984; Evans and Parsegian, 1986; Evans, 1991; McIntosh et al., 1989c; McIntosh and Simon, 1993), or protrusions of individual lipid molecules (Israelachvili and Wennerström, 1990, 1992).

For the past several years there has been considerable interest in determining the effects that exogenously added molecules have on these attractive and repulsive interactions, and consequently on bilayer adhesion. For electrically neutral phosphatidylcholine (PC) bilayers the interbilayer fluid space can be increased, and consequently the adhesion energy decreased, by the addition of fatty acids, which increase electrostatic repulsion (McIntosh and Simon, 1996); ketocholesterol, which increases the hydration pressure (Simon et al., 1992); the ganglioside GM1, which

Received for publication 30 May 1996 and in final form 12 September 1996.

Address reprint requests to Dr. Sidney A. Simon, Department of Neurobiology, Duke University Medical Center, Durham, NC 27710. Tel.: 919-684-4178; Fax: 919-684-4431; E-mail: sas@neuro.duke.edu.

0006-3495/96/12/3261/17 $2.00

increases the steric and electrostatic repulsion between headgroups (McIntosh and Simon, 1994b); and lysolecithin, which increases the undulation pressure (McIntosh et al., 1995). The interbilayer fluid spacing can be decreased, and the adhesion energy increased, by the addition of large polymers (such as polyethyleneglycol) that do not adsorb to the membrane surface but increase the osmotic pressure in the bulk phase relative to the interbilayer space (Parsegian et al., 1979, 1986; Evans, 1991). However, as most molecules that induce adhesion between membranes bind to or are attached to them, it follows that if they were to decrease the fluid spacing they would have to decrease one or more of the nonspecific repulsive pressures, increase the attractive van der Waals pressure, or, like adhesion molecules, form bridges between the bilayers.

We decided to investigate polyphenolic molecules as possible candidates for molecules that can increase the adhesion between biological surfaces. Of the naturally occurring polyphenols, tannic acid (TA) (see Fig. 1) was originally chosen to be investigated because it precipitates or complexes with a variety of macromolecules, including alkaloids, polymers, polysaccharides, cyclodextrins, and proteins having H-bond acceptors (Haslam et al., 1989). Such proteins include proline-rich proteins found in saliva (Glendinning, 1992). Moreover, proline-rich proteins found in spider webs (Andersen, 1970; Guerette et al., 1996) and 3,4-dihydroxybenzene-rich proteins secreted by barnacles (Waite, 1983) are involved in important adhesion processes for these animals. Polyphenols such as tannic acid appear to associate with macromolecules by simultaneously donating many hydrogen bonds to H-bond-accepting groups (Haslam et al., 1989) and by hydrophobic interactions arising from the aromatic rings on its gallic acids (Oh et al., 1980). The hydrophobic interaction ensures that TA interacts at interfacial regions where the dielectric constant is lower than in bulk solution, so that the H bonds that form are stronger than they would be in water (Nowick et al., 1994; Shan et al., 1996).

Early studies of the effects of tannic acid on bilayers were performed to understand its fixative properties, especially with phosphatidylcholines (Kalina and Pease, 1977). Kalina and Pease suggested that TA interacts with the choline

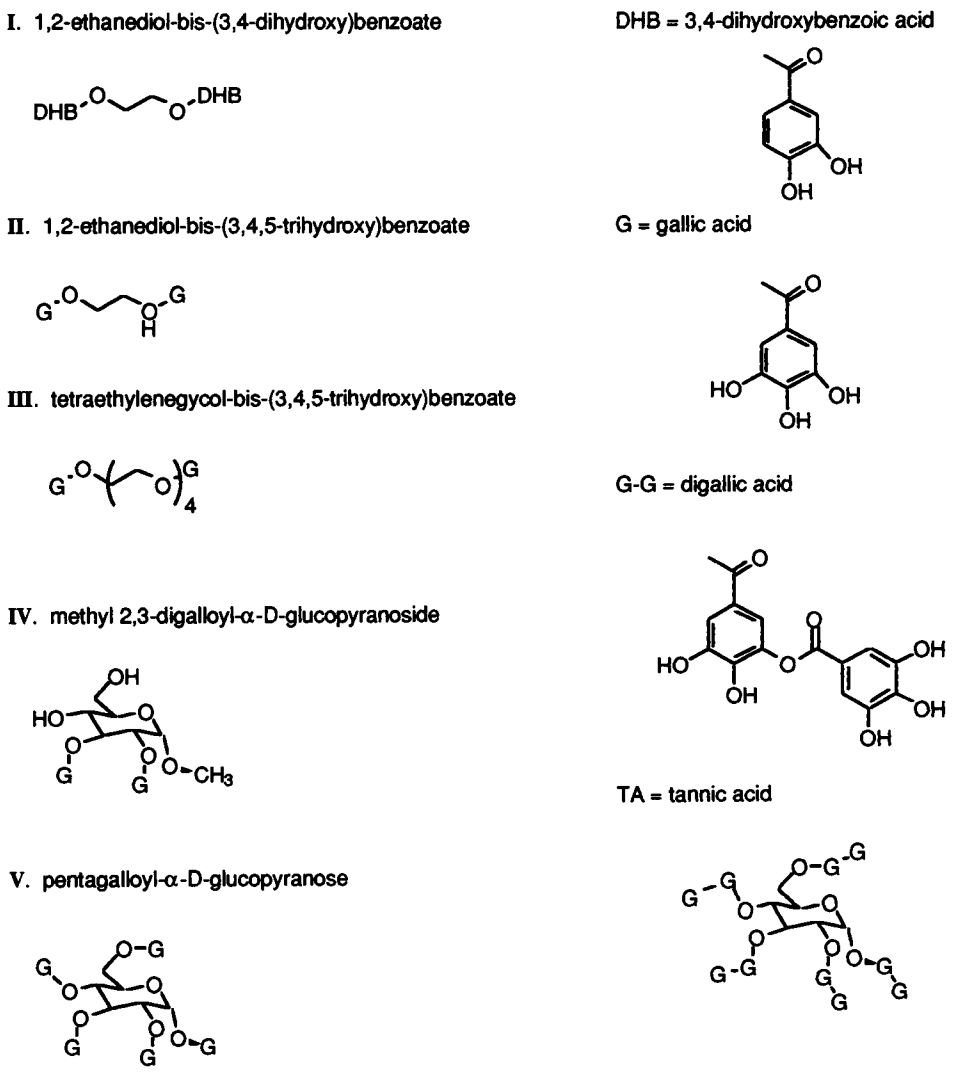

FIGURE 1 Chemical structures of the five polyphenols synthesized (compounds I–V).

group of PC to form a "complex" that can be stabilized against dehydration and then stained with OsO_4. Under these fixed conditions they found that multilayers of dipalmitoylphosphatidylcholine (DPPC) have a periodicity of 45 Å, which is significantly less than the repeat period of 64 Å obtained from x-ray measurements in excess water (Tardieu et al., 1973; McIntosh, 1980). In addition, Schrijvers et al. (1989) found that in thin sections egg phosphatidylcholine (EPC) fixed with TA has a periodicity of 48 Å, which is markedly reduced from its repeat period of 63 Å obtained from x-ray measurements in excess water (Tardieu et al., 1973; LeNeveu et al., 1977; McIntosh and Simon, 1986b). Schrijvers et al. (1989) also found that when high concentrations of TA are added to small unilamellar vesicles, the vesicles break to form multilayers. X-ray diffraction measurements showed that TA decreases the fluid spacing between gel and liquid crystalline PC bilayers to about 5 Å (Simon et al., 1994). Based on x-ray diffraction, NMR, and monolayer data, we (Simon et al., 1994) hypothesized that TA decreases the interbilayer fluid spacing by forming bridges between apposing bilayers.

Although TA (molecular weight 1701) is a relatively simple molecule compared with adhesion proteins, analyses of its interaction with lipids are nevertheless quite complicated because TA contains five digallic acid moieties, each covalently bonded to a D-glucose (Fig. 1). In this regard we do not know what characteristics a polyphenol must possess to markedly reduce the fluid spacing between bilayers. For example, it is not known how many gallic acids are required or even if the digallic acid moieties are essential. To learn which characteristics may be important, we analyze in this paper a variety of smaller and simpler polyphenols that have either been synthesized or bought from commercial sources. Compounds were tested that vary in their overall length and number and/or orientation of their hydroxyl groups. In this regard, it was found that in investigating the interaction of polyphenols with β-galactosidase that the greater the number of gallic acid residues on the central glucose, the lower the concentration needed for precipitation (Haslam, 1974; Haslam et al., 1989). To test whether a particular polyphenol mimics the effects of TA in reducing the fluid spacing between PC bilayers, we investigate D-methyl gallate and the following compounds, the structures of which are given in Fig. 1: compound I (two dihydroxybenzoic acids linked by ethylene glycol); compound II (two gallic acids linked by ethylene glycol); compound III (two gallic acids linked by tetraethylene glycol), the extended length of which is comparable to that of TA; compound IV (gallic acids in the 2 and 3 positions of D-glucose), and compound V (five gallic acids covalently bound to D-glucose).

EXPERIMENTAL PROCEDURES

Materials and methods

EPC and dipalmitoylphosphatidylcholine (DPPC) were purchased from Avanti (Alabaster, Al) and used without further purification. Salts were reagent grade. The following chemicals were purchased from Aldrich (Milwaukee, WI): methyl gallate (methyl 3,4,5-trihydroxybenzoate) (98%), oxalic acid, 3,4-dihydroxybenzoic acid, *t*-butyldimethylchlorosilane, imidazole, gallic acid, tertaethylene glycol, tetrabutylammonium fluoride, benzyl chloride, dimethylaminopyridine, 4,6-*O*-(benzyldiene)methyl-α-D-glucopyranoside, and trifluoroacetic acid. Tannic acid was purchased from Fluka Chemical Company (Buchs, Switzerland). To purify the TA, it was dissolved in a small amount of ethanol and a large amount of ether. The solid materials were removed by filtration, and after evaporation a pale yellow powder was obtained with a melting point of 209.4°C, in good agreement with the literature value for TA (Weast, 1984). Polyvinylpyrrolidone (PVP) (average MW 40,000 (x-ray) and 3,000 (monolayer)) was purchased from Sigma Chemical Co. Water was passed through organic and ion exchange filters. Unless otherwise stated, 100 mM NaCl, 1 mM HEPES at pH 7.0 was used as our standard buffer.

Synthesis of compounds

All solvents were distilled before use. Reactions were run in flame-dried glassware under nitrogen. Proton nuclear magnetic resonance (^{1}H NMR) spectra were obtained on a Varian XL-300 spectrometer. Chemical shifts are reported in ppm downfield from tetramethylsilane (TMS) with residual solvent such as $CDCl_3$ as an internal standard. Melting points were obtained on a Thomas-Hoover capillary melting point apparatus and were uncorrected.

The compounds given Roman numerals were synthesized for the purpose of investigating their effects on phosphatidylcholine monolayers and bilayers. However, to achieve this other compounds required as synthetic intermediates were also prepared.

tert-Butyldimethylsilyl-3,4,-(bis-tert-butyldimethylsilyloxy)benzoate

The compounds 3,4-dihydroxybenzoic acid (5.25 g), *tert*-butyldimethylchlorosilane (15.39 g), and imidazole (9.28 g) were dissolved in 350 ml of dimethylformamide (DMF) and stirred at 25°C for 12 h. After the reaction was completed, 150 ml of water was added. The oil phase was extracted twice with 400 ml ether. The extracts were pooled; washed with 5% $NaHCO_3$, 5% HCl, and water; and then dried over $MgSO_4$. The drying agent was removed by filtration, and the solvent was evaporated to produce a yellow oil that solidified upon cooling. This solid was purified by flash chromatography with 5% EtOAc in hexane (R_f = 0.45) and gave 15.8 g, 93% of the theoretical yield of *tert*-butyldimethylsilyl-3,4,-(bis-*tert*-butyldimethylsilyloxy)benzoate. The melting point (m.p.) of this compound was 144–146°C. ^{1}H NMR ($CDCl_3$, ppm): 7.59 (dd, J = 8.4, 2.1 Hz, ^{1}H; Ar-6-**H**), 7.55 (d, J = 2.1 Hz, ^{1}H; Ar-2-**H**), 6.85 (d, J = 8.1 Hz, ^{1}H; Ar-5-**H**), 0.98 (s, 18 **H**), 0.97 (s, 9 **H**), 0.21 (s, 12 **H**), 0.20 (s, 6 **H**).

1,2-Ethanediol bis-3,4-di(tert-butyldimethylsilyloxy)benzoate

Ten grams of *tert*-butyldimethylsilyl-3,4,-(bis-*tert* butyldimethylsilyloxy) benzoate was added to 30 ml CH_2Cl_2 containing 5 drops of DMF and 2.7 ml of oxalyl chloride added dropwise at room temperature. After stirring for 2 h at room temperature, the solvent was evaporated and the residual oily product was dissolved in 50 ml of $CHCl_3$ and evaporated twice to give 3,4-bis(*tert*-butyldimethylsilyloxy)benzoyl chloride in quantitative yield. ^{1}H NMR ($CDCl_3$, ppm): 7.61 (dd, J = 8.4, 2.4 Hz ^{1}H; Ar-6-**H**), 7.54 (d, J = 2.4 Hz, ^{1}H; Ar-2-**H**; 6.85 (J = 8.4, ^{1}H; Ar-5-**H**), 0.95 (s, 9 H; 4-Si-C($\mathbf{CH_3}$)$_3$), 0.94 (s, 9 H; 3-Si-C($\mathbf{CH_3}$)$_3$), 0.21 (s, 6 H; 4-Si-C($\mathbf{CH_3}$)$_2$), 0.20 (s, 6 H; 3-Si-C($\mathbf{CH_3}$)$_2$). This compound was then dissolved in 30 ml $CHCl_3$ and 2.9 g *N,N*-dimethylaminopyridine and 0.51 ml anhydrous ethylene glycol added dropwise at room temperature. After 12 h the solution was poured into 200 ml of water and extracted twice with 200 ml ether. The extract was dried over $MgSO_4$, filtered, and condensed to give a viscous, milky oil. This oil was purified by flash column chromatography

(5% EtOAc in hexane, R_f = 0.32) to give 6.05 g 1,2-ethanediol bis-3,4-di(*tert*-butyldimethylsilyloxy)benzoate (85% yield) as a white solid with a melting point of 79–80°C. ^{1}H NMR ($CDCl_3$, ppm): 7.55 (d, J = 2.1 Hz, 2 H; Ar-2**H**), 7.52 (m, 2 H; Ar-6**H**), 6.81 (d, J = 8.1 Hz, 2 H; Ar-5**H**), 4.58 (s, 4 H; CO_2CH_2), 0.96 (s, 18 H; 4-Si-C(CH_3)$_3$), 0.95 (s, 18 H; 3-Si-C(CH_3)$_3$), 0.20 (s, 12 H; 4-Si-(CH_3)$_2$), 0.19 (s, 12 H; 3-Si-(CH_3)$_2$).

1,2-Ethanediol bis-3,4-(dihydroxy)benzoate (compound I, Fig. 1)

1,2-Ethanediol bis-3,4-di(*tert*-butyldimethylsilyloxy)benzoate (3.76 g) was dissolved in 20 ml THF. To this solution, 10 ml tetrabutylammonium fluoride was added portionwise, and 4 ml 48% HF was added to keep the pH between 5.0 and 8.0. The solution was stirred at room temperature until completion (2 h) as judged by TLC (R_f = 0.0; 2:1 hexane:EtOAc). The solution was then poured into a separatory funnel containing 200 ml of 5% $NaHCO_3$ and 100 ml of ether. The organic phase was washed with water, dried over $MgSO_4$, filtered, and condensed to give 1.5 g 1,2-ethanediol bis-3,4-(dihydroxy)benzoate (95% yield) as a pale yellow powder with a melting point of 226–228°C. ^{1}H NMR (d_6-acetone, ppm): 8.64 (s, 2 H; 4-Ar-O**H**), 8.33 (s, 2 H; 3-Ar-O**H**), 7.51 (d, J = 2.1 Hz, 2 H; Ar-2-**H**) 7.46 (dd, J = 8.4, 2.1 Hz, 2 H; Ar-2-**H**), 6.88 (d, J = 8.4 Hz, 2 H; Ar-5-**H**) 4.58 (s, 4 H; CO_2CH_2).

tert-Butyldimethylsilyl-3,4,5-(tris-tert-butyldimethylsilyloxy)benzoate

The same method was employed as in the preparation of *tert*-butyldimethylsilyl-3,4,-(bis-*tert*-butyldimethylsilyloxy)benzoate. This compound had a melting point of 83–84°C and was characterized using ^{1}H NMR ($CDCl_3$, ppm) by the following parameters: 7.22 (s, 2 H; Ar-2, 6-**H**), 1.0 (s, 9 H; CO_2-Si-C(CH_3)$_3$), 0.98 (s, 9 H; 4-Si-C(CH_3)$_3$), 0.92 (s, 18 H; 3, 5-Si-C(CH_3)$_3$), 0.35 (s, 6 H; CO_2-Si(CH_3)$_2$, 0.23 (s, 12 H; 3, 5-Si(CH_3)$_2$), 0.12 (s, 6 H; 4-Si-(CH_3)$_2$).

3,4,5-(Tris-tert-butyldimethylsilyloxy)benzoic acid

tert-Butyldimethylsilyl-3,4,5,-(tris-*tert*-butyldimethyl-silyloxy) benzoate (12.55 g at room temperature) was dissolved in 50 ml THF containing 10 ml DMF and 30 ml 1 N HCl. After the solution was stirred for 3 h, 100 ml water was added, and the compound was extracted twice with 200 ml ether. The extract was pooled, dried over $MgSO_4$, filtered, and condensed to give a white powder. The solid was then dissolved in a minimum amount of EtOAc and purified by flash column chromatography (2:1 hexane:EtOAc; R_f = 0.25) to give 9.85 g (96%) 3,4,5-(tris-*tert*-butyl dimethylsilyloxy-)benzoic acid. This compound had a melting point of 223–224°C. ^{1}H NMR ($CDCl_3$, ppm): 7.29 (s, 2 H; Ar-2,6-**H**), 1.02 (s, 9 H; 4-Si-C(CH_3)$_3$), 0.97 (s, 18 H; 3,5-Si-C(CH_3)$_3$), 0.25 (s, 12 H; 3,5-Si(CH_3)$_2$), 0.17 (s, 6 H; 4-Si(CH_3)$_2$).

1,2-Ethanediol bis-3,4,5-tri(tert-butyldimethylsiloxy)benzoate

3,4,5-(Tris-*tert*-butyldimethylsilyloxy)benzoic acid (5 g) was converted to the corresponding benzoyl chloride using the same method as in the synthesis of 1,2-ethanediol bis-3,4-di(*tert*-butyldimethylsilyloxy)benzoate (see above). 1,2-Ethanediol bis-3,4,5-tri(*tert*-butyl-dimethyl siloxy)benzoate was prepared as described for the preparation of 1,2-ethanediol bis-3,4-di(*tert*-butyldimethylsilyloxy)benzoate. That is, after waiting 2 days for the reaction to be completed, 200 ml water was added, and the compound was extracted twice with 200 ml ether. The organic layer was washed and evaporated, and the product was then purified by flash column chromatography (5% EtOAc in hexane, R_f = 0.42) to give 3.25 g 1,2-ethanediol bis-3,4,5-tri(*tert*-butyldimethylsiloxy)benzoate (65% yield). 1,2-Ethanediol bis-3,4,5-tri (*tert*-butyldimethylsiloxy)benzoate has a melting point of 98–99°C and was characterized using ^{1}H NMR ($CDCl_3$, ppm): 7.23 (s, 4 H; Ar-2,6-**H**): 4.56 (s, 4 H; CO_2CH_2): 1.0 (s, 18 H; 4-Si-C(CH_3)$_3$): 0.92 (s, 36 H; 3,5-Si-C(CH_3)$_3$): 0.22 (s, 24 H; 3,5-Si(CH_3)$_2$): 0.14 (s, 12 H; 4-Si(CH_3)$_2$).

1,2-Ethanediol bis-3,4,5-trihydroxybenzoate (compound II, Fig. 1)

A solution containing 3.25 g 1,2-ethanediol bis-3,4,5-tri(*tert*-butyldimethylsiloxy)benzoate was treated as described in the synthesis of compound I. After the reaction was completed, the solution was poured into 100 ml water and extracted five times with 100 ml ether containing 10% THF. The solvents were evaporated, and the remaining solid was then dissolved in 5 ml boiling EtOH to which 200 ml ether was added. The precipitated *tert*-butyl dimethylsilane salt was removed by filtration. Finally, hexane was added to the above solution to obtain a colorless oily precipitate that upon drying transformed into 0.903 g of a white amorphous powder (85% yield). Compound II had a melting point of 273–274°C. ^{1}H NMR (d_6-DMSO, ppm): 7.27 (s, 4 H; Ar-2, 6-**H**): 4.45 (s, 4 H; CO_2CH_2).

Tetraethyleneglycol bis-3-4-5-tri(tert-butyldimethylsilyloxy)benzoate

Starting with 5 g 3,4,5-(tris-*tert*-butyldimethylsilyloxy)benzoic acid and using the same methods as described for the preparation of 1,2-ethanediol bis-3,4,5-tri(*tert*-butyldimethyl siloxy)benzoate, we prepared tetraethyleneglycol bis-3-4-5-tri(*tert*-butyldimethylsilyloxy) benzoate. This compound was purified by flash column chromatography (5% EtOAc in hexane, R_f = 0.35) to give 3 g of the oily product (52% yield). ^{1}H NMR (d_6-DMSO, ppm): 7.22 (s, 4 H; Ar-2,6-**H**), 4.40 (t, J = 4.1, 4 H; $CO_2CH_2CH_2$), 3.80 (t, J = 4.0, 4 H; CO_2CH_2), 3.67 (m, 8 H; $CH_2CH_2OCH_2CH_2$), 0.97 (s, 18 H; 4-Si-C(CH_3)$_3$), 0.93 (s, 36 H; 3,5-Si-C(CH_3)$_3$), 0.22 (s, 24 H; 3,5-Si(CH_3)$_2$), 0.13 (s, 12 H; 4-Si(CH_3)$_2$).

Tetraethyleneglycol bis-3,4,5-trihydroxybenzoate (compound III, Fig. 1)

The same methods that were employed for the preparation of compound II were used to prepare 1.1 g compound III (87% yield; m.p. = 29–30°C). ^{1}H NMR (d_6-DMSO, ppm): 6.95 (s, 4 H; Ar-2,6-**H**), 4.27 (d, 4 H; $CO_2CH_2CH_2$), 3.68 (d, 4 H; CO_2CH_2), 3.53 (d, J = 7.5, 8 H; $CH_2CH_2OCH_2CH_2$).

Methyl-2,3-di-(tri-O-benzyl)galloyl-4,6-O-benzylidene-α-D-glucopyranoside

To 30 ml $CHCl_3$ was added 2.35 g (+)-(4,6-*O*-benzylidene)methyl-α-D-glucopyranoside, 5 ml pyridine, 0.5 g dimethylaminopyridine and 9.17 g 3,4,5-tri-*O*-benzylgalloyl chloride, and the resulting solution was then stirred at 61°C for 4 days. The resulting solution was diluted with 150 ml $CHCl_3$ and then washed in a separatory funnel successively with 200 ml water, saturated $CuSO_4$, 0.05 M HCl, water, and dilute $NaHC0_3$. The solvent was then evaporated and the residue was dissolved in EtOAc and purified using flash column chromatography with EtOAc:hexane 1:2.5 as the solvent system (R_f = 0.48). The solvent was evaporated to yield 5.82 g (62% yield) of a white solid (methyl-2,3-di-(tri-*O*-benzyl)galloyl-4,6-*O*-benzylidene-α-D-glucopyranoside) with a m.p. = 180–180.5°C. This compound was characterized by ^{1}H NMR ($CDCl_3$) by the following parameters: 7.35 (m, 39 H, Ar), 6.07 (t, ^{1}H, C-3), 5.60 (s, ^{1}H; benzylidene), 5.28 (t, ^{1}H; C-1), 5.19 (t, ^{1}H, C-2), 4.90–5.10 (m, ^{1}H; C-4), 4.12 (m, ^{1}H, C-5), 3.93 (m, 2 H; C-6), 3.48 (s, 3 H; CH_3).

Methyl 2,3-di-(tri-O-benzyl)galloyl-α-D-glucopyranoside

Methyl-2,3,-di-(tri-*O*-benzyl)galloyl-4,6-*O*-benzylidene-α-D-glucopyranoside (5.4 g) was dissolved in 25 ml dichloromethane, 2.5 ml trifluoroacetic acid, and 0.5 ml water at room temperature. After 5 min the mixture was diluted with 75 ml dichloromethane and washed with saturated $NaHCO_3$, and then with water. The solution was then dried over $MgSO_4$ and evaporated to obtain 4.58 g (92% yield) of methyl 2,3,-di-(tri-*O*-benzyl)galloyl-α-D-glucopyranoside. This white waxy compound had R_f = 0.23 in EtOAc: hexane (1:1). ^1H NMR ($CDCl_3$): 7.36 (m, 34 H; phenyl), 5.77 (t, ^1H; C-3), 5.21 (t, ^1H; C-1), 5.16 (m, ^1H, C-2), 4.95–5.07 (m, 12 H; benzyl), 4.03 ((t, ^1H; C-4), 3.98 (m, 2 H; C-6), 3.97 (m, ^1H, C-5), 3.47 (s, 3 H; CH_3).

Methyl-2,3-di-galloyl-α-D-glucopyranoside (compound IV, Fig. 1)

Methyl-2,3,-di-(tri-*O*-benzyl)galloyl-α-D-glucopyranoside (4 g) in 50 ml THF was reduced with hydrogen at room temperature over 10% palladized charcoal for 12 h. The solution was then filtered through Cellite powder, the filtrate was then evaporated and redissolved in EtOAc, and hexane was added to yield a precipitate that was dried to give 1.75 g (91% yield) of a white powder, methyl 2,3-di-galloyl-α-D-glucopyranoside. This compound had a m.p. = 241–244°C. ^1H NMR (DMSO): 6.83 (m, 4 H; gallic phenol), 5.44 (t, 1 **H**; C3), 4.84 (m, 1 **H**; C-1), 4.81 (m, 1 **H**; C-2), 3.98 (m, 2 H; C-6), 3.614 (m, 1 **H**; C-5), 3.266 (s, 3 **H**; CH_3).

Penta-O-galloyl-α-D-glucose (compound V, Fig. 1)

This compound was prepared using the procedure of Armitage et al. (1961).

Absorbance measurements

Large unilamellar vesicles (LUVs) (~0.1 μm diameter) were formed from multilamellar lipid vesicles (MLVs) by the freeze-thaw high-pressure extrusion method (Hope et al., 1985). In brief, EPC (3 mg) in excess water (6 ml) was vortexed to form MLVs. MLVs were then freeze-thawed six to eight times and extruded through 0.1-μm polycarbonate filters in 100 mM buffer 10–20 times. The final lipid concentration was 1 mg/ml within 10% error, as determined by independent phosphate concentration measurements. Absorbance measurements of these dispersions were performed at 25°C on a dual-beam Shimadzu spectrophotometer at a wavelength of 560 nm in a thermostatted cuvette stirred with a small magnetic stirring bar. The reference cell contained only buffer. With the exception of TA and glucose, which were in buffer, small aliquots of concentrated stock solutions of the other compounds in methanol were added to the cuvette with a Hamilton syringe. In control measurements these small concentrations of methanol (a few microliters) did not significantly affect the absorbance of LUVs. Only steady-state changes in absorbance are reported.

Polyphenol binding measurements

The number of polyphenols bound to EPC vesicles that resulted in a significant increase in absorbance was determined by obtaining the total lipid concentration and the free polyphenol concentration. The total phosphate concentration was obtained by a modified Bartlett procedure. The free polyphenol concentration was obtained by first forming LUVs of EPC at 1 mg/ml as described above. Polyphenols at various concentrations were then added, and the suspension was vortexed and centrifuged at 5000 rpm for 2 h through ultracentrifuge filter units with a 0.22-μm pore size (PGC Scientific Gaithersberg, MD). In separate experiments without lipid present we found that the polyphenols, namely PGG and TA, passed completely through the filter. The filtrates were washed with $CHCl_3$ to remove the small amount of lipid that passed through the filter. The concentrations of TA and PGG in the filtrates were then obtained by UV spectrometry.

Microelectrophoresis

The electrophoretic mobility (μ) for EPC vesicles was measured at 25°C with a Rank Brothers Mark I apparatus using methods described previously (Simon et al., 1994). Approximately 0.1 mg of lipid per 10 ml of buffer (100 mM NaCl in 1 mM HEPES at pH 7.0) was vortexed for about 1 min to obtain a uniform-looking dispersion. The zeta potential (ζ) was calculated using the Helmholtz-Smoluchowski equation, which at 25°C reduces to $\zeta = 12.85\ \mu$, where μ is in $\mu m\ s^{-1}/V\ cm^{-1}$ (Hunter, 1986).

Differential scanning calorimetry

Samples were prepared by codissolving DPPC with individual polyphenols (usually with methanol) at various mole fractions. The solvent was evaporated, placed in a stainless steel calorimeter sample pan, and weighed. The standard buffer (100 mM NaCl, 1 mM HEPES at pH 7.0) was added to the sample pan at about four times the weight of the lipid, and the pan was then sealed. The lipid dispersion was heated to 55°C (above its transition temperature) for about 2 h, allowed to cool to room temperature, and placed in a Perkin-Elmer DSC7 calorimeter, where it was heated at 2°C/min. The reference cell contained only buffer. The samples were heated and cooled until the same scans were obtained on successive heating cycles.

Dipole potential measurements

Dipole potentials (V) were measured as described previously (MacDonald and Simon, 1987; Simon et al., 1991). Monolayers were formed by spreading 10 μl of a 10 mg/ml lipid in hexane:ethanol (9:1 v/v) solution onto a subphase of 0.1 M NaCl, 1 mM HEPES (pH 7.0) in a trough with a surface area of about 20 cm^2. The solution was stirred with a small Teflon-coated magnetic flea. Under these conditions the packing of the lipid molecules in the monolayer is approximately the same as it is in multilayers (MacDonald and Simon, 1987). The dipole potential was measured at room temperature between a Ag/AgCl electrode in the subphase and a ^{241}Am electrode in air using a electrometer (model 602; Keithley Instruments Co., Cleveland, OH). The values of V represent the difference in the potential of the subphase surface in the presence and absence of the lipid monolayer. Changes in the dipole potential (ΔV) produced by polyphenolic compounds were obtained by injecting them into the subphase from stock solutions having the same salt concentrations as the subphase. Those polyphenols that were sparingly soluble in water were dissolved in methanol. The amount of methanol injected into the subphase did not affect the dipole potential.

X-ray diffraction

X-ray diffraction analysis was performed on unoriented suspensions of multiwalled vesicles and on oriented multilayers in controlled humidity atmospheres. Three methods were used to prepare the suspensions. In the first method, used for most experiments, solutions of the various polyphenols (Fig. 1) were added to LUVs as described for the absorbance measurements. In the second method excess buffer containing the polyphenols was added to dry lipid so that multilamellar vesicles were formed. To ensure equilibration of the salt across the multilayers, several freeze-thaw cycles were used. The first and second methods gave very similar results. In the third method, the lipids and polyphenols were codissolved in methanol at specific mole ratios, the solvent was evaporated, the excess buffer was added, and the suspension was vortexed and allowed to incubate above the lipid's phase transition temperature. For each method, the suspensions were pelleted with a bench centrifuge, sealed in quartz glass x-ray capillary tubes, and mounted in a point collimation x-ray camera. Oriented multilayers were formed by placing a drop of the methanolic solution of lipid and polyphenol on a curved glass surface and removing the methanol under a stream of nitrogen. The resulting oriented multilayers

were mounted in a controlled humidity chamber on a line-focus x-ray camera as described previously (McIntosh et al., 1987, 1989a).

X-ray diffraction patterns were recorded on Kodak DEF x-ray film. The films were processed by standard techniques and densitometered with a Joyce-Loebl microdensitometer as described previously (McIntosh and Simon, 1986b; McIntosh et al., 1987, 1989a). After background subtraction, integrated intensities, $I(h)$, were obtained for each order h by measuring the area under each diffraction peak. For unoriented patterns, the structure amplitude $F(h)$ was set equal to $\{h^2I(h)\}^{1/2}$ (Blaurock and Worthington, 1966; Herbette et al., 1977). Electron density profiles, $\rho(x)$, on a relative electron density scale were calculated from

$$\rho(x) = (2/d)\sum \exp\{i\phi(h)\} \cdot F(h) \cdot \cos(2\pi xh/d), \quad (1)$$

where x is the distance from the center of the bilayer, d is the lamellar repeat period, $\phi(h)$ is the phase angle for order h, and the sum is over h. Phase angles for EPC and DPPC bilayers containing PGG were determined by comparing the observed structure amplitudes to the continuous transforms previously observed for EPC and DPPC, respectively (McIntosh et al., 1983; McIntosh and Simon, 1986b). The resolution ($d/2h_{max}$) of the profiles was 6–8 Å.

RESULTS

Absorbance and binding measurements

Fig. 2 shows the absorbance changes at 560 nm (A_{560}) produced by the addition of compounds I-V, TA, methyl gallate, and glucose to EPC LUVs in 0.1 M NaCl buffer. Compound V (PGG; *open circles*) and TA (*filled circles*) produced sigmoidal increases in absorbance, with the half-maxima increases occurring at about 10 μM. At the highest concentrations these dispersions had a milky appearance ($A_{560} \approx 2$). Compound IV (*open squares*) also produced large increases in A_{560}, but required about a 100-fold higher concentration than for TA or PGG. The absorbance data for compounds I, II, and III tracked those of IV until 10^{-3} M (not shown). At higher concentrations these compounds aggregated in solution and contributed to the light scattering and thus were not useful in characterizing the changes in absorbance arising from their interaction with EPC LUVs. Two water-soluble polyhydroxylated compounds, glucose and methyl gallate, did not produce significant changes in A_{560} (Fig. 2). These two compounds were of interest because glucose forms the central core of IV, V, and TA, and methyl gallate, in the form of gallic acid, is covalently bound to the glucose moiety in IV, V, and TA. The experiments with glucose and methyl gallate show that simply increasing the osmotic pressure did not lead to a significant increase in absorbance.

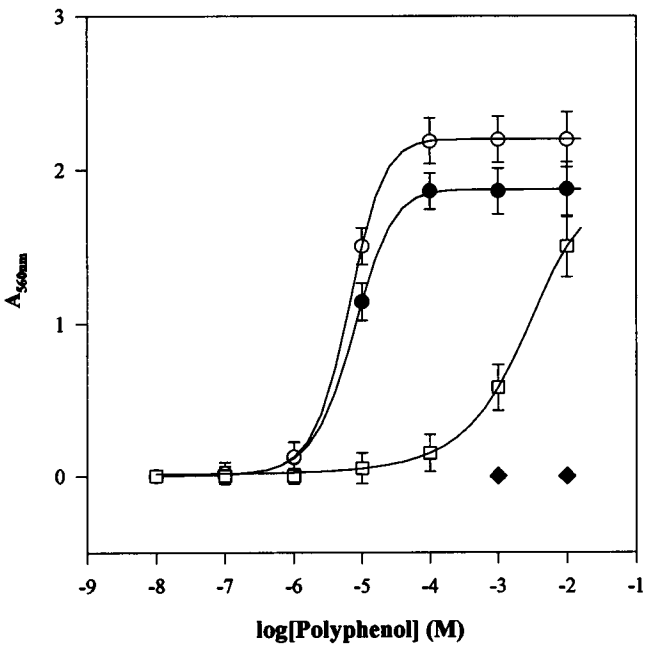

FIGURE 2 Absorbance changes in LUVs of egg phosphatidylcholine vesicles produced by the addition of polyphenols. The steady-state changes in absorbance (ΔA at 560 nm) are plotted against the polyphenol concentration. Tannic acid (●) and compound V (PGG; ○) both dramatically increase the absorbance of the LUVs. Compound IV (□) is about 100 times less effective. The diamonds represent the responses produced by methyl gallate or by glucose. The lines connecting the points have no theoretical meaning.

The number of EPC molecules per compound V (PGG) and TA bound were obtained at concentrations that produced large increases in absorbance (10^{-5}, 10^{-4}, and 5×10^{-4} M). Under these conditions the mole ratios of EPC:PGG and EPC:TA were (mean of two experiments) 153:1 and 177:1 at 10^{-5} M, 20.4:1 and 20.2:1 at 10^{-4} M, and 4.75:1 and 4.63:1 at 5×10^{-4} M. That is, at the bulk concentration that produced the greatest increase in absorbance, the mole ratio of EPC to bound PGG or TA was about 20:1.

Dipole potential

Traces of dipole potential readings for EPC and DPPC in the absence and presence of polyphenols are shown in Fig. 3 *A*. As shown in the top trace, spreading liquid crystalline phase EPC over the buffer subphase increased V by 410 ± 20 mV. Injection of PGG into this subphase decreased V in a concentration-dependent manner up to a concentration of 10^{-4} M. At higher concentrations the change in dipole potential (ΔV) remained approximately constant some 380 mV below the baseline of 410 mV (Fig. 3 *A, top trace*). Injection of 2% and 4% PVP, a polymer known to precipitate TA (Nash et al., 1966), partially reversed the PGG decrease in dipole potential. This reversibility suggests that PVP, by mass action, caused some of the PGG to be desorbed from the monolayer. As shown in the bottom trace, spreading DPPC over the buffer subphase at a temperature where DPPC multilayers would be in a gel phase increased the dipole potential to 550 ± 15 mV. The addition of PGG to the subphase reduced V in a concentration-dependent manner, but the maximum decrease in V was about 250 mV. Injection of 4% PVP completely reversed the PGG-induced decrease in dipole potential, again suggesting that by mass action the adsorbed PGG desorbed from the monolayer, thus increasing the dipole potential.

Fig. 3, *B* and *C*, presents the changes in V produced by the polyphenols I-V, TA, and methyl gallate on monolayers of

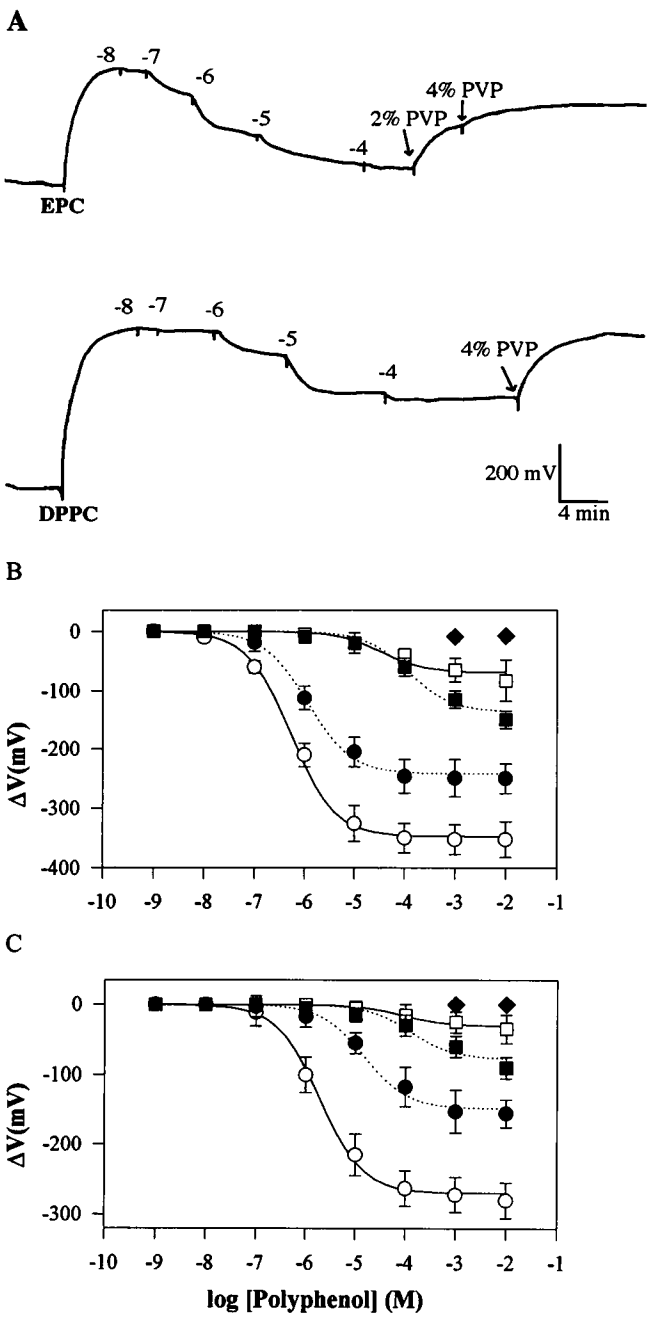

FIGURE 3 (*A*) Dipole potential changes produced by polyphenols. *Upper trace:* Monolayer of EPC spread over a subphase of 0.1 M NaCl, 1 mM HEPES (pH 7) produced a 410-mV increase in dipole potential. Injections of PGG in the stirred subphase at indicated concentrations (M) produced decreases in the dipole potential. When the dipole potential reached steady state after the 10^{-4} M injection, 2% and 4% PVP were injected into the subphase (*arrows*). *Lower trace:* Same experiment as above, except that the monolayer was DPPC. Scale bar refers to both experiments. (*B* and *C*) Mean changes in dipole potential (ΔV) of polyphenols injected into the subphase below monolayers of EPC (*B*) and DPPC (*C*). Methyl gallate (♦); compounds I, II, and III (□); IV (■); PGG (○); and tannic acid (●). The lines were fit to Langmuir isotherms (see text).

EPC and DPPC, respectively. For these polyphenols the changes in dipole potential with polyphenol concentration (ΔV) were well fit by a Langmuir isotherm (*solid lines*): $\Delta V/\Delta V_{max} = 1/\{1 + K_d/\{Conc\}\}$, where K_d is the apparent dissociation constant and ΔV_{max} is the maximum change in dipole potential. Plotted in this manner, the changes in ΔV are pronounced only in the concentration range encompassing $\approx \pm 10\ K_d$. For EPC the maximum changes in dipole potential produced by polyphenols were −347 mV for compound V (PGG); −245 mV for TA; −136 mV for compound IV; −70 mV for compounds I, II, and III; and approximately 0 mV for methyl gallate (Fig. 3 *B* and Table 1). For TA the changes in dipole potential were similar to those reported previously for TA that was not recrystallized (Simon et al., 1994). For DPPC (Fig. 3 *C*) similar trends for ΔV_{max} and K_d were found for the different polyphenols, although they had smaller magnitudes (Table 1). For all of the tested compounds the values for K_d and ΔV_{max} are given in Table 1.

Differential scanning calorimetry

Thermograms of DPPC liposomes prepared at various mole ratios of PGG (*left panel*) and TA (*right panel*) are shown in Fig. 4 *A*. In excess buffer, DPPC exhibited two well-characterized endothermic transitions. The first is a pretransition with a peak temperature at 35°C, and the second is the main transition (T_m) with a peak temperature of 41.1°C. The enthalpy of main endothermic transition was 8.3 ± 0.63 kcal/mol. These values are in agreement with those in the literature (Cevc and Marsh, 1987). The addition of PGG at mole ratios as low as 50:1 eliminated the pretransition and slightly lowered the T_m of the main endothermic transition. At mole ratios of 20:1 the thermograms consisted of two endothermic transitions. At even higher mole ratios (10:1 and 5:1) the peak widths decreased and T_m remained constant at about 38°C. The thermal behavior of TA was similar to that of PGG in that T_m was lowered and the transition width was increased (20:1) and then decreased at the higher concentrations (e.g., 5:1).

Fig. 4 *B* shows plots of the mean changes in the transition temperature (T_m) and enthalpy (ΔH_m) as a function of the

TABLE 1 Apparent binding constants of polyphenols to EPC and DPPC monolayers

Lipid	Polyphenol	K_a (μM)	ΔV_{max} (mV)
EPC	I	35	70
	II	35	70
	III	35	70
	IV	100	136
	PGG (V)	0.53	347
	TA	1.2	245
DPPC	I	85	30
	II	85	30
	III	85	30
	IV	124	77
	PGG (V)	1.96	269
	TA	15.0	148

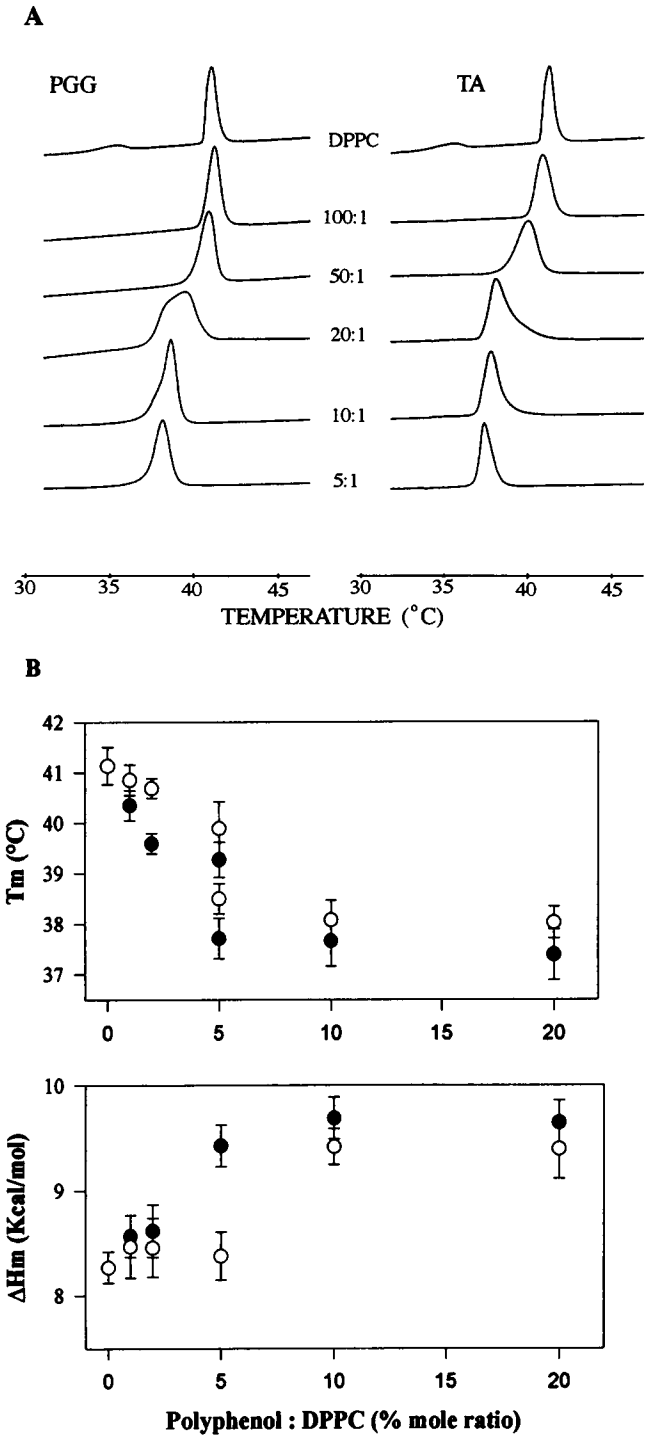

FIGURE 4 (*A*) Thermograms of DPPC liposomes at various mole ratios of PGG (*left traces*) and tannic acid (TA) (*right traces*). Endothermic transitions are upward. (*B*) Graphs of transition temperatures (T_m) and transition enthalpies (ΔH_m) plotted versus percentage mole ratio of DPPC: PGG (○) and DPPC:TA (●). The half-filled circles represent DPPC in excess buffer. The data represent the mean ± SE of at least four trials.

mole ratios of PGG:DPPC (*open circles*) and TA:DPPC (*filled circles*) ($N = 3$). Below 5 mol% PGG/DPPC the main endothermic transition decreased linearly. At 5 mol% two endothermic transitions were observed (Fig. 4 *A*). At mole ratios between 10 and 20 mol% (PGG/DPPC), only one transition temperature at 37.5°C was present. For TA/DPPC dispersions (*filled circles*), T_m decreased linearly by about 2°C from 0 to 2% mole ratio. At 5 mol% two endothermic transitions were observed. From 5 to 20% mole ratio, T_m remained nearly constant. For PGG-DPPC dispersions ΔH_m remained constant at about 8.4 kcal/mol up to 5% mole ratio. For mole ratios greater than 10% ΔH_m increases to 9.5 kcal/mol. For TA, ΔH_m abruptly increased from 8.4 kcal/mol at 2 mol% to 9.5 kcal/mol at 5% mole ratio, where it remained at this enthalpy up to 20% mole ratio.

The thermograms of DPPC with compounds I, II, and III were, within experimental error, the same in that T_m decreased slightly with increasing polyphenol concentration (to 39.5°C at 20 mol%), and the enthalpies remained unchanged (data not shown). For compound IV the transition temperature decreased to about 39.5°C at 20% mole ratio and the transition enthalpy remained constant up to 15% mole ratio, whence it increased about 1 kcal/mol at 20% mole ratio (data not shown).

Microelectrophoresis

To determine whether the binding of TA or PGG imparted fixed charges to the EPC bilayer, we measured the electrophoretic mobility (μ) of EPC vesicles in 0.1 M NaCl, 1 mM HEPES (pH 7.0) at different TA and PGG concentrations. Uncharged lipid vesicles do not respond to a DC electric field and hence have a negligible value of μ (Tatulain, 1983). As described in Materials and Methods, the zeta potential can be calculated from the electrophoretic mobility using $\zeta = 12.85\ \mu$. For EPC in the standard buffer, ζ was essentially 0 mV, as was found by others (Tatulain, 1983). Two problems arose in measuring the electrophroetic mobility of EPC liposomes with PGG and TA. The first is that the particles aggregated and they constantly had to be vortexed to break up the dispersion. The second is that vesicle population did not have a uniform size or a homogeneous mobility. For liposomes on the order of 20 μm, ζ was 16.3 ± 2.1 mV (0.01 mM PGG) and −15 .8 ± 1.8 mV (0.1 mM PGG). For TA we confirmed our previous measurements using TA that was not recrystallized (Simon et al., 1994) and found that from 1 μ M to 1 mM, ζ remained constant at about −19 mV (although, as before, this preparation was also heterogeneous). We also performed a titration curve of 1 mM TA in 0.1 M NaCl (not shown). The titration curve is S-shaped, having two regions where the slope of the pH versus moles base/moles TA were approximately constant. The constant slope regions were between $2.8 \leq \text{pH} \leq 3.8$, and $6.8 \leq \text{pH} < 8.5$. The latter undoubtedly represents the titration of the phenolic groups (Gustavson, 1956). Thus at pH 7, at which all of our experiments were performed, TA is negatively charged. The electrophoresis and titration studies show that these two polyphenols impart a negative charge to PC liposomes, and by electrostatic repulsion, should cause them to increase their fluid spacing.

X-ray diffraction

As observed previously (McIntosh and Simon, 1986b), the x-ray diffraction patterns of EPC suspensions consisted of several low-angle reflections that indexed as orders of a single lamellae repeat period of 63 Å and a broad wide-angle pattern centered about 4.5 Å, and patterns of DPPC suspensions consisted of several low-angle reflections that indexed as orders of a single lamellae repeat period of 64 Å and wide-angle patterns that contained a sharp reflection at 4.21 Å and a broad reflection centered at 4.08 Å. The patterns from EPC are typical of bilayers in the liquid-crystalline ($L\alpha$) phase, and the patterns from DPPC are typical of bilayers in the gel ($L\beta'$) phase, where the hydrocarbon chains are tilted with respect to the plane of the bilayer (Tardieu et al., 1973).

For EPC bilayers the addition of compounds I-III, even at quite high concentrations, did not markedly alter the lamellar repeat period. For liposomes formed from a 5:1 mole ratio of EPC to compounds I, II, or III, the lamellar repeat was 62 ± 1 Å. At a mole ratio of 2:1 EPC:compound III, the repeat period decreased to 60 Å. The repeat periods of LUV in 10^{-2} M solutions of compounds I, II, or III were 61–62 Å.

Compound IV produced somewhat larger changes in the spacings of EPC LUVs; in 10^{-3} M, 5×10^{-3} M, and 2×10^{-2} M solutions of compound IV the lamellar repeat periods were 65 Å, 58 Å, and 57 Å, respectively. Freeze-thawed MLVs in 10^{-3} M compound IV produced a single repeat at 61 Å, but in 10^{-2} M compound IV produced two repeat periods, at 63 Å and 56 Å, with the reflections more intense in the 63-Å repeat (data not shown).

The lamellar repeat period decreased significantly at high concentrations of compound V (PGG). Fig. 5 shows the repeat period of EPC suspensions plotted against the logarithm of the concentration of PGG (*open circles*) and TA (*filled circles*). For PGG concentrations up to 10^{-4} M the repeat period remained nearly constant at 63 Å. However, at a critical concentration of about 5×10^{-3} M there was a sharp decrease in repeat period of over 10 Å. Experiments performed using dispersions in which PGG was added to LUVs showed single repeat periods, either 63 ± 1 Å (at a concentration of 2.5×10^{-4} M) or 51 ± 2 Å for higher concentrations. However, in one experiment in which the multilamellar liposomes containing 10^{-3} M PGG were produced by the freeze-thaw method, the patterns indicated the existence of two phases (Fig. 5): one with weak reflections indexing on a lamellar repeat period of 63 Å and the other with more intense reflections indexing as orders of a repeat period of 50 Å. As shown previously (Simon et al., 1994), TA exhibited a similar behavior (Fig. 5).

X-ray patterns of unoriented 10:1 EPC:PGG dispersions in excess water gave a repeat period of 59 Å. Oriented samples of 10:1 EPC:PGG gave repeat periods that decreased monotonically from 49 Å at 98% relative humidity (compared to 52 Å in the absence of PGG) to 47 Å at 32% relative humidity (compared to 50 Å in the absence of PGG). Thus, in excess water, and for all relative humidities, the repeat periods of 10:1 EPC:PGG were 3–4 Å smaller than the repeat periods of EPC recorded under the same conditions (McIntosh et al., 1987).

Electron density profiles were calculated to determine the changes in the widths of the bilayer and the interbilayer fluid spacings caused by the incorporation of the polyphenols, especially PGG, which had the greatest effect on the lamellar repeat period. The structure amplitudes for EPC bilayers in the presence of PGG were similar to those for EPC (Fig. 6), indicating that the phase combination previously obtained for EPC (McIntosh and Simon, 1986b) also applied to EPC bilayers containing PGG. Electron density profiles of fully hydrated EPC bilayers in water and in 10^{-3} M PGG are presented in Fig. 7. For each profile two unit cells are shown containing two apposing bilayers and the

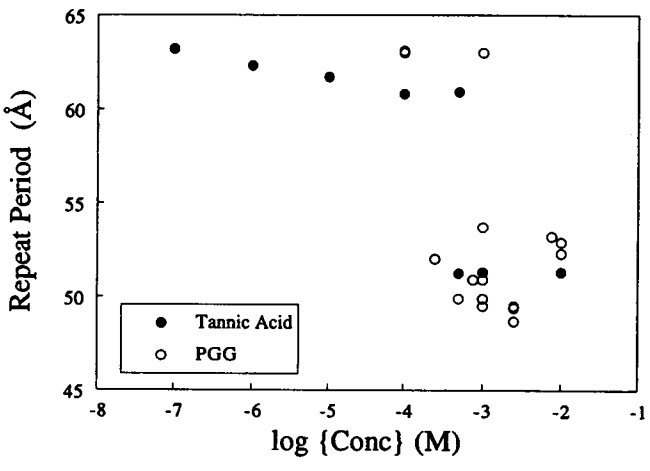

FIGURE 5 Repeat period for liposomes of EPC plotted versus concentration of PGG (○) and TA (●). Data for TA taken from Simon et al. (1994).

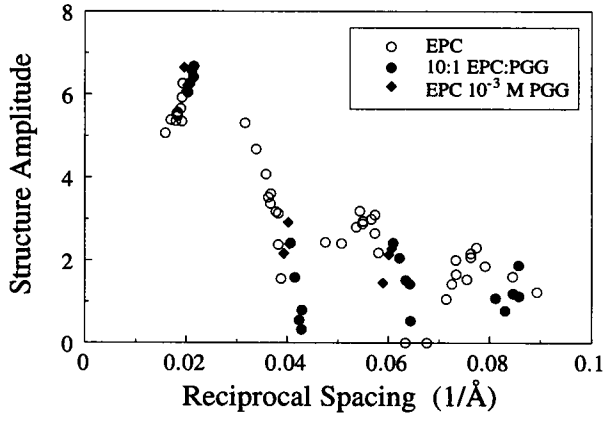

FIGURE 6 Structure amplitudes for bilayers of EPC, 10:1 EPC:PGG, and EPC in excess 10–3 M PGG. The structure amplitudes for EPC, taken from McIntosh and Simon (1986b), represent a range of repeat periods obtained with a series of applied osmotic pressures. The structure amplitudes for 10:1 EPC:PGG were obtained for samples in excess water and at different relative humidity atmospheres.

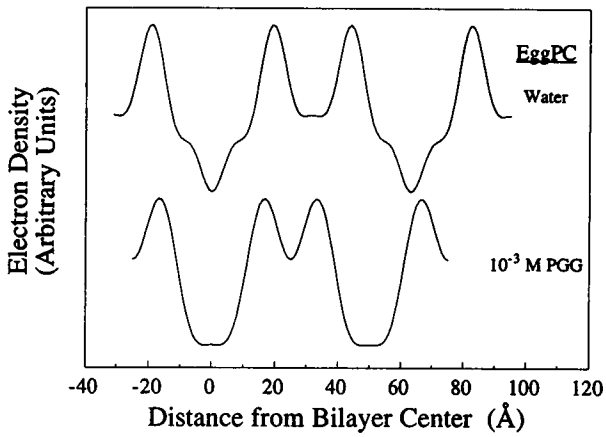

FIGURE 7 Electron density profiles of EPC (*upper trace*) and EPC:PGG bilayers in excess buffer and 10^{-3} M PGG.

intervening fluid space. For each profile the bilayer on the left is centered at the origin, so that the low-density trough at 0 Å corresponds to the terminal methyl groups in the bilayer center. For EPC in water the high-density peaks centered near ±20 Å correspond to the EPC headgroups, the medium-density regions between the headgroup peaks and the terminal methyl trough correspond to the methylene chains, and the medium-density region centered about 32 Å corresponds to the middle of the fluid layer between adjacent bilayers. These profiles show that PGG altered three structural features. First, the distance between the headgroup peaks across the bilayer decreased by about 3 Å, indicating that the bilayers became thinner in the presence of PGG. Second, the terminal methyl trough disappeared as the electron density in the bilayer center became more uniform. Third, the width of the fluid space between apposing bilayers decreased by about 10 Å in the presence of PGG.

Profiles such as those shown in Fig. 7 can be used to estimate the distance between apposing bilayers at each polyphenol concentration. As noted previously (McIntosh et al., 1987, 1989a; McIntosh and Simon, 1986b), the definition of the lipid/water interface is somewhat arbitrary, because the bilayer surface is not smooth and water penetrates into the headgroup region of the bilayer. We operationally define the bilayer width as the total physical thickness of the bilayer, assuming that the conformation of the phosphorylcholine headgroup in these bilayers is the same as it is in single crystals of phosphatidylcholine. In that case the high-density headgroup peak would be located between the phosphate group and the glycerol backbone (Lesslauer et al., 1972). We assume that the phosphorylcholine group is, on average, oriented approximately parallel to the bilayer plane, so that the edge of the bilayer lies about 5 Å outward from the center of the high-density peaks in the electron density profiles (McIntosh et al., 1987; McIntosh and Simon, 1986b). Therefore, for each polyphenol concentration we calculate the bilayer thickness as the distance between headgroup peaks across the bilayer in the profiles plus 10 Å. The distance between bilayer surfaces (d_f) is calculated as the difference between the lamellar repeat period and this bilayer thickness.

Using these definitions, we found for oriented 10:1 EPC:PGG bilayers in relative humidity atmospheres that the bilayer thickness was 3–4 Å smaller than for EPC at the same humidity. Thus, for bilayers in controlled humidity atmospheres, where the fluid space between bilayers was very small (1 to 4 Å; McIntosh et al., 1987), the observed decrease in repeat period caused by the addition of PGG was due almost entirely to a decrease in bilayer thickness. However, for dispersions in excess buffer, the presence of PGG reduced the width of both the bilayer and the interbilayer fluid space. For EPC in suspensions containing PGG concentrations of 10^{-3} M or more, the average bilayer thickness was 45.0 ± 1.7 Å (mean ± standard deviation, $N = 7$ experiments), compared to 47.8 ± 0.8 Å ($N = 10$) for EPC in water (McIntosh and Simon, 1986b). The change in fluid layer thickness caused by PGG in suspensions of EPC is shown in Fig. 8. The fluid spacing remained approximately constant until a critical concentration was attained, and then it abruptly decreased by about 10 Å. At higher PGG concentrations the fluid spacing remained approximately constant at about 5 Å. Because of limited resolution, we were unable to construct electron density profiles at 10^{-4} M PGG. However, because the repeat period of 63 Å was the same as for EPC in excess buffer, we assumed that d_f remained unchanged. With this assumption we also found a sharp decrease in fluid spacing at a critical concentration of TA (Fig. 8).

For EPC bilayers formed with compound IV we obtained only one pattern with high enough resolution ($h = 3$) to construct electron density profiles and thereby calculate the fluid space. This pattern ($d = 61$ Å) was obtained for a freeze-thawed sample containing 10^{-3} M compound IV. Under these conditions the bilayer thickness decreased by about 1.5 Å and the fluid space decreased by about 1 Å.

In the gel phase of DPPC, the addition of compounds I, II, or III increased the lamellar repeat period by about 7 Å.

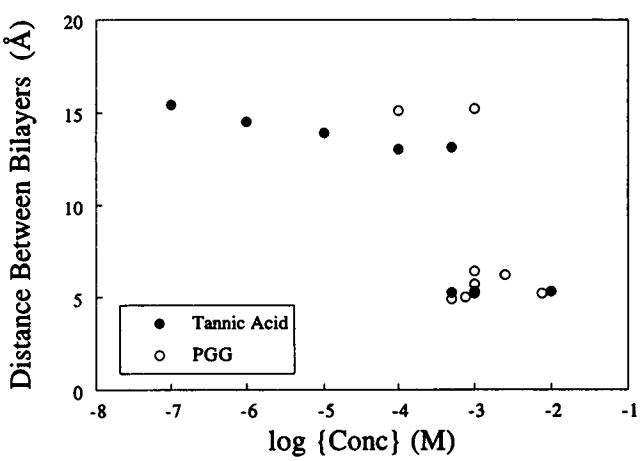

FIGURE 8 Fluid spacing between EPC bilayers plotted against the PGG (○) and tannic acid (●) concentrations. (TA data from Simon et al., 1994).

That is, suspensions of 5:1 mole ratios of DPPC to compound I, II, or III gave a lamellar repeat period of 71 ± 1 Å, and a single sharp wide-angle reflection at 4.12 Å. Both the lamellar repeat periods and wide-angle spacing are typical of gel-phase DPPC bilayers with untilted hydrocarbon chains (Tardieu et al., 1973; McIntosh, 1980). The increase in repeat period from 64 Å for DPPC to 71 Å for DPPC with compounds I, II, or III can be explained completely by the increase in bilayer thickness caused by a loss of chain tilt (McIntosh, 1980; Tardieu et al., 1973). Therefore, the addition of these high concentrations of compounds I, II, or III had no appreciable effect on the width of the interbilayer fluid spacing.

Suspensions of 10:1 DPPC:compound V (PGG) gave a very different x-ray pattern, with a 46 Å lamellar repeat period and a single, sharp 4.09-Å wide-angle reflection. The structure factors for 10:1 DPPC:PGG bilayers (data not shown) fell on the continuous transform previously observed for DPPC in the interdigitated phase (McIntosh et al., 1983). Electron density profiles of DPPC and 10:1 DPPC:PGG bilayers are shown in Fig. 9. One unit cell containing a single bilayer is shown in each profile, with the center of each bilayer at 0 Å. There are pronounced differences between these profiles. First, the headgroup peaks for DPPC are located at ±21 Å, and the headgroup peaks for DPPC:PGG are located at ±15 Å, indicating that the bilayer thickness is decreased by about 12 Å by the addition of PGG. Second, although there is a prominent terminal methyl trough in the center of the DPPC bilayer, there is no trough in the center of the DPPC:PGG bilayer, indicating that the terminal methyl groups are not localized in the center of the bilayer containing PGG. The electron density profile and the wide-angle reflection show that the 10:1 DPPC:PGG bilayer is in an interdigitated phase, where the hydrocarbon chains from apposing monolayers interpenetrate (McIntosh et al., 1983; Ranck et al., 1977; Simon and McIntosh, 1984). Third, and most importantly for our subsequent analysis, using the definition of bilayer thickness given above we find that PGG reduced the fluid space of DPPC from 12 Å in excess buffer (in the $L\beta'$ phase) to about 6 Å. Thus PGG collapsed the fluid space in both gel and liquid crystalline bilayers.

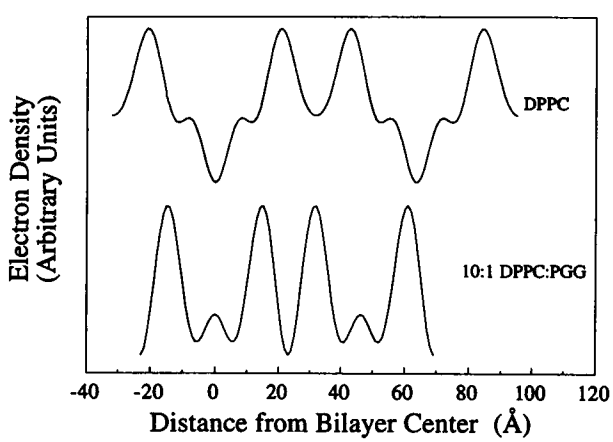

FIGURE 9 Electron density profiles of fully hydrated DPPC and 10:1 DPPC:PGG bilayers.

DISCUSSION

The data presented in this paper provide information on the interaction of several newly synthesized polyphenolic analogs of tannic acid with liquid crystalline EPC and gel-phase DPPC bilayers. Of the analogs tested, only PGG behaved like tannic acid in increasing the absorbance (Fig. 2), decreasing the dipole potential (Fig. 3), increasing the transition enthalpy (Fig. 4), and markedly decreasing the fluid spacing between adjacent bilayers (Fig. 8). We now discuss these results and present arguments as to why only PGG, of the polyphenols tested, mimicked the behavior of tannic acid.

Absorbance

The large increases in absorbance of EPC LUVs induced by micromolar concentrations of PGG and TA (Fig. 2) are likely the consequence of vesicle-vesicle aggregation and/or vesicle rupture to form multilamellar vesicles at the higher concentrations (Schrijvers et al., 1989; Simon et al., 1994). The formation of vesicle aggregates and/or liposomes results in larger particles that scatter more light (Day et al., 1980). When the dispersions produced by the addition of PGG to EPC LUVs were analyzed by x-ray diffraction, they showed sharp reflections indicative of the presence of multiwalled liposomes, thus providing good evidence that upon the asymmetrical addition of large concentrations of PGG the LUVs ruptured and aggregated to form MLVs. The increase in absorbance could not be caused by the addition of any polyhydroxylated osmolite, because neither 10^{-2} M glucose nor 10^{-2} M methyl gallate (in 0.1 M NaCl) produced significant absorbance changes (Fig. 2). Micropipette experiments (Needham et al., 1990) have shown that EPC unilamellar vesicles will rupture when the area of one monolayer of the bilayer increases by 3–4% without a corresponding area increase in the apposing monolayer. In our experiments, preformed LUVs could break with the addition of polyphenols if their diffusion across the bilayer was sufficiently slow as to be unable to compensate for the area increase of the outside monolayer. Previously, we found this to be the mechanism by which TA ruptures giant unilamellar vesicles (Simon et al., 1994). It is important to note that the changes in absorbance produced by the polyphenols were seen at a lower concentration than the changes in repeat period recorded on dispersions prepared in the same manner. That is, at 10^{-4} M PGG, where absorbance was a maximum (Fig. 2), the repeat period did not change from its control value of 63 Å. This suggests that at 10^{-4} M PGG, the absorbance increase was a consequence of the breaking of LUVs to form MLVs (or at least larger particles) rather than any specialized adhesive interaction of the polyphenols that would lead to a collapse of the interlamellar fluid space.

Compound IV produced large increases in absorbance, but about 100 times larger concentrations were required than that for PGG or TA (Fig. 2). The x-ray measurements indicate that this absorbance increase was also a consequence of the breakage of LUVs to form MLVs. Compounds I–III also produced changes in absorbance, but because they aggregated in solution at higher concentrations, light scattering measurements will be needed to interpret these data.

Differential scanning calorimetry

When solutes form dilute solutions in the gel and liquid crystalline phases, the changes in transition temperature can be written (Kaminoh et al., 1988) as

$$dT_m^{pp}/d\{PP\}_t = (K^g - K^{lc})/\{C + D(K^{lc} + K^g)\}, \quad (2)$$

where T_m^{pp} is the transition temperature for a given polyphenol concentration, $\{PP\}_t$ is the total polyphenol concentration in the dispersion, the K's are the membrane-water partition coefficients in the gel (g) and liquid crystalline (lc) phases, and C and D are constants. At low mole ratios both PGG and TA decreased T_m. From Eq. 2 this decrease arises because of a greater partitioning of the polyphenols into the liquid-crystalline than into the Lβ or Lβ' gel phases. This conclusion is also consistent with the apparent binding constants obtained from dipole potential measurements in EPC and DPPC monolayers (Table 1). The data in Fig. 5 *B* show that, as a function of increasing polyphenol concentration, T_m decreased more abruptly with TA than with PGG, suggesting that TA has a slightly higher partition coefficient in the liquid crystalline phase than PGG. At high mole ratios T_m is independent of the concentration of PGG or TA, which indicates (see Eq. 2) that the partition coefficients are approximately the same in both gel and liquid crystalline phases. At high mole ratios the x-ray data show that both polyphenols induce interdigitated (LβI) gel phases in DPPC (Fig. 8 and Simon et al., 1994). To rationalize why the partition coefficients are similar in the Lα and LβI phases in spite of the fact that the interdigitated phase is a gel phase (and hence K would be expected to be smaller), we note that the area per molecule is approximately the same in these two phases (70–76 Å^2; see below). Therefore because the polyphenols partition primarily in the headgroup region, the interactions with the bilayer are likely to be similar. Note also that interdigitated phases cannot occur in monolayers, so the binding constants measured in solid DPPC monolayers (Table 1) may be different than for interdigitated bilayers.

Utilizing the fact that PGG and TA form interdigitated phases, we interpret the phase diagrams (Fig. 4 *B*) at low mole fractions (<5% for TA and <10% for PGG) to represent phase transitions from the Lβ' or Lβ to the Lα phase, and at high mole fractions (>15 mol%), to represent phase transitions from interdigitated (LβI) phases to the Lα phase. At the high mole fractions the decrease in width of the phase transition, together with the larger ΔH_m, is also indicative of the LβI to Lα phase transition (McIntosh et al., 1984; Swarmy and Marsh, 1995). The reason for the decrease in transition width and higher ΔH_m is that, as evidenced by the wide-angle diffraction, the hydrocarbon chains in the interdigitated phase are more closely packed than in the Lβ' gel phase (Simon and McIntosh, 1984). Therefore in the interdigitated phase there is a larger van der Waals interaction between hydrocarbon chains that gives rise to a larger transition enthalpy and a more cooperative phase transition (McIntosh et al., 1984). Compound IV also showed an abrupt increase in ΔH_m at 20% mol ratio, suggesting that it may form an interdigitated phase, although this was not tested by x-ray diffraction because of our limited supply of this compound.

The thermograms obtained with PGG or TA differed from those obtained for other compounds capable of H bonding with DPPC. For example, ethanol produces a biphasic effect on T_m, with small concentrations of ethanol decreasing T_m and large concentrations increasing T_m when the interdigitated phase is formed (Simon and McIntosh, 1984)). Glycine, proline, and betane all increase T_m and do not markedly change ΔH_m (Rudolph and Goins, 1991). Finally, 1 M sucrose produces very small changes in T_m and ΔH_m (Chowdhy et al., 1984), whereas complete replacement of water with glycerol induces an interdigitated phase but does not markedly change T_m (McDaniel et al., 1983; Swarmy and Marsh, 1995)

The DPPC thermograms show that, over the entire concentration range tested, compounds I, II, and III slightly reduced T_m without appreciably changing ΔH_m. Based on Eq. 2, this behavior suggests that these compounds have larger partition coefficients in the liquid crystalline than in the gel phase. The x-ray data indicate that the major structural change produced by these compounds was to remove the tilt of the acyl chains, thus inducing a Lβ gel phase. Apparently they do not accumulate to a significant volume fraction in the interface to induce an interdigitated phase.

A final point regarding these data is that at the highest concentrations of PGG and TA, where the fluid spacing is about 5Å, the transition temperature differs by only a few °C from the transition temperature in excess water. This suggests that the bilayers behave as if they were fully hydrated, because dehydrating them markedly increases T_m by virtue of a decrease in molecular area and a increase in van der Waals interactions between the acyl chains (Cevc and Marsh, 1987). Despite the decrease in fluid spacing, this dehydrated state is prevented because when PGG partitions into the interface it increases the molecular area (see below), and because the hydroxyl groups on each gallic acid can substitute for the interfacial H-bonded waters.

Association of polyphenols with monolayers and bilayers

For uncharged PC monolayers, it has been shown experimentally as well as by molecular dynamics simulations that

the dipole potential (V) arises from the dipole in the PC headgroup and compensating water dipoles (Simon and McIntosh, 1989; Zhang and Vanderkooi, 1992; Brockman, 1994). In other words, the dipole potential represents the difference between two very large potentials—one produced by the polarized water molecules and the other by the lipid dipoles (Marrink et al., 1993). Which of these two factors is more important in rationalizing the reduction of the dipole potential caused by polyphenols cannot be obtained by these experiments.

All of the polyphenols tested produced larger reductions in the dipole potential (ΔV) for liquid-expanded EPC monolayers than for solid DPPC monolayers. For PGG this difference was approximately 100 mV (380 mV to 280 mV) and cannot be attributed simply to a greater surface density of polar headgroups, bnecause at 20°C the molecular area of EPC is greater than for DPPC. The differences likely arise from different interfacial locations of the polyphenols in these monolayers, because it would take more work for them to intercalate into the solid DPPC chain than fluid EPC chains, which are reflected in the different binding constants of the polyphenols in these two phases (Table 1). This interpretation is also consistent with the calorimetry experiments, which indicate that $K^{lc} > K^{g}$. The polyphenols are not the only chaotropic compounds (water structure breakers) that bind better to the liquid crystalline than to the gel phase of PC. For example, the chaotropic anion tetraphenylboron also binds better to the liquid crystalline than to the gel-phase bilayers (Smejek and Wang, 1990).

For monolayers of EPC and DPPC, the values of K_d and ΔV_{max} produced by methyl gallate and compounds I–IV were much less than those for PGG and TA (Table 1). This can be partially rationalized by the greater number of polyphenol residues per molecule (which is 10 for TA, 5 for PGG, 2 for Compounds I–IV, and 1 for methylgallate) that can be associated with the monolayer. The relatively small differences between compounds IV and compounds I, II, and III may reside in the fact that they all have two polyphenolic moieties. The data in Fig. 3, *B* and *C*, and Table 1 indicate that polyphenols decreased the dipole potential to various extents, depending on their concentration and chemical structure. In this sense they behave like biologically active polyhydroxlated compounds such as phloretin and its analogs (Reyes et al., 1983).

Structural changes and localization of polyphenols in PC bilayers

For EPC bilayers, the x-ray measurements show that PGG decreased the bilayer thickness by about 3 Å. A similar result was previously found for TA (Simon et al., 1994). We argue that the decrease in thickness occurs because PGG (as well as many other surface active molecules) partitions into the interfacial region and wedges apart the lipid molecules to accommodate one or more of its gallic acids. To keep the density in the bilayer approximately constant, the acyl chains accommodate by decreasing the mean bilayer thickness (Simon et al., 1994). The increase in area is reflected in the electron density profile as a delocalization of the terminal methyl groups (Fig. 7). A broadened terminal methyl trough has also been observed for other lipids with large areas per molecule, such as the polyunsaturated lipid DAPC, which has a molecular area of 76 Å^2 (McIntosh et al., 1995). From the observed thickness changes in the electron density profiles, the area per molecule for EPC bilayers in the presence of PGG can be estimated by the following calculation. If PGG partitioned only into the interfacial region of EPC, and if the volume change is much less than the area change, then $\Delta A/A_o = -1/(1 + L_o/\Delta L)$, where A_o (64 Å^2) and L_o (28 Å) are the area/molecule and hydrocarbon thickness in the absence of PGG, respectively (McIntosh and Simon, 1986b; McIntosh et al., 1987). For EPC-PGG bilayers, ΔA = 6.2 Å^2, which corresponds to a molecular area of 70.2 Å^2.

For gel-phase DPPC bilayers, the polyphenols reduced or eliminated chain tilt (compounds I–III) or caused the acyl chains to fully interdigitate (PGG and TA). Decreasing the chain tilt is a consequence of compounds I–III partitioning into the interfacial regions and consequently increasing the area per molecule, and thereby reducing the "in-plane" steric interactions between the relatively bulky PC headgroups that give rise to acyl chain tilt (McIntosh, 1980). The simplest way of reducing the in-plane steric interactions is for the headgroup to rotate out of the plane of the bilayer. To induce acyl chain interdigitation amphipathic molecules must take up a greater volume fraction of the interfacial region. In 10:1 DPPC:PGG bilayers, where an interdigitated phase is formed, an appreciable volume fraction of the interfacial region must be occupied by the gallic acids of PGG because 1) not much of the volume of PGG ("diameter" ≈ 16 Å; see Fig. 9) can be accommodated in the narrow (5–6 Å) fluid space between bilayers, and 2) the size of PGG (molecular weight 940) is large compared to that of the PC headgroup (molecular weight 300).

It has previously been shown that other H-bonding amphipathic compounds, such as ethanol, benzyl alcohol, glycerol, and heptanetriol, can partition into the interfacial region and increase the molecular area in the liquid-crystalline phase and induce hydrocarbon chain interdigitation in the gel phase (McIntosh et al., 1983; Simon and McIntosh, 1984; Simon et al., 1988). However, none of these other amphipathic compounds reduce the interbilayer fluid separation as observed in the case of PGG in both the liquid-crystalline phase (Fig. 7) and the gel phase (Fig. 8). PGG reduced the fluid space between adjacent EPC bilayers to about 5 Å (Fig. 7), a distance corresponding to the width of two water molecules, and where steric interactions are observed, between EPC headgroups from apposing bilayers (McIntosh et al., 1987). To illustrate further how small a 5-Å fluid spacing is, we note that the equilibrium fluid spacing for subgel phase DPPC bilayers is approximately 3 Å larger (8.3 Å) than for PGG-EPC. In the subgel phase, where the lipid hydrocarbon chains are crystallized, the

entropic undulation and protrusion forces are thought to be very small (McIntosh and Simon, 1993). Therefore, PGG decreases the fluid space to a greater extent than occurs by eliminating virtually all out-of-plane steric repulsive pressures (McIntosh and Simon, 1993). We now consider the question of mechanism.

Effect of polyphenols on attractive and repulsive interactions between bilayers

Because PGG reduces the fluid spaces between adjacent bilayers, it must either increase the attractive pressure(s) or decrease the repulsive pressures between bilayers. The interbilayer pressures between electrically neutral PC bilayers include the attractive van der Waals pressures and repulsive steric and hydration pressures (Rand and Parsegian, 1989; McIntosh and Simon, 1993, 1994a). The important point is that only two equilibrium fluid spacings were observed for the PGG-EPC bilayers (Fig. 7). The two equilibrium fluid spaces can be represented in a potential energy diagram by two distinct minima representing the different adhesion energies in these states (Lipowski, 1994). The smaller one, at $d_f \approx 15$ Å, is found at zero and low PGG concentrations and has an adhesion energy of -0.013 erg/cm^2 (Evans, 1994). This energy is determined by a balance between the attractive van der Waals pressure and the repulsive hydration and steric pressures (Evans and Parsegian, 1986; McIntosh and Simon, 1993, 1994a). The energy minimum at 5 Å represents a larger (because the surfaces are closer), but unknown, adhesion energy. Previous analysis has shown that for EPC bilayers, the work needed to decrease d_f from 15 Å to 5 Å is about 0.5 erg/cm^2 (McIntosh and Simon, 1986). These two energy minima must be separated by an energy barrier that arises from the work: energy required to overcome the repulsive undulation and hydration pressures (0.5 erg/cm^2), an electrostatic repulsive pressure arising from the adsorption of negatively charged PGG to the bilayers, and any steric pressures arising from the intercalated PGG molecules. Thus once a critical concentration of PGG is bound, the free energy gain is sufficiently large to overcome the barrier, so that the bilayers fall into a very deep and narrow potential well at a fluid spacing of 5 Å.

We now consider the possibility that PGG alters one or more of the attractive and repulsive pressures in a manner consistent with it decreasing the fluid spacing over a narrow concentration range (Fig. 8). The possibility that the polyphenols and the lipids compete for the same limited supply of water, thus making less water of hydration available, is eliminated because absorbance and x-ray measurements were performed on dispersions in excess water. Therefore the reduction in the fluid spacing results from the direct interaction of the polyphenols with the bilayers. The possibility that PGG causes the fluid space to decrease by decreasing the undulation pressure is unlikely for two reasons. First, in liquid-crystalline EPC bilayers PGG decreased the bilayer thickness (Fig. 8), which should decrease the bending modulus and increase the undulation pressure (Simon et al., 1995). Second, in interdigitated gel phase bilayers, where the undulation pressure should be small (Evans, 1991; McIntosh and Simon, 1993, 1994a), PGG also collapsed the fluid spacing (Fig. 8). The possibility that PGG increases the van der Waals pressure must be considered because PGG partitions into the headgroup, and headgroup-headgroup interactions (as apposed to the van der Waals interactions between the acyl chains) are the primary attractive interaction responsible for the small fluid spacing and large adhesion energy between lipids such as digalactosyldiacylglycerol (Attard et al., 1988; Evans and Needham, 1988). However, if PGG were only increasing the van der Waals pressure, then the repeat period should decrease continuously as a function of the volume fraction of PGG, rather than with the abrupt decrease that is experimentally observed (Fig. 8).

We next consider how the polyphenols could affect the repulsive hydration pressure (P_h). This pressure has been shown to decay exponentially as $P_h = P_o \exp(-d_f/\lambda)$, where P_o is its magnitude and λ is its decay length (LeNeveu et al., 1977; McIntosh et al., 1989a; McIntosh and Simon, 1986b; Parsegian et al., 1979). Several studies have correlated P_o with V^2, where V is the dipole potential (McIntosh et al., 1989b; Simon and McIntosh, 1989; Simon et al., 1992). Because PGG markedly reduces the dipole potential (Fig. 3), it would be expected to decrease the hydration pressure. However, the argument against using the decrease in dipole potential as the primary cause for decrease in d_f is that the dipole potential decreases monotonically from 10^{-8} M to 10^{-5} M PGG (Fig. 3 *B*), whereas the fluid space decreases abruptly at a concentration of about 10^{-3} M PGG (Fig. 8).

Therefore, because neither an increased van der Waals nor decreased repulsive hydration/steric pressures can completely explain the observed sharp decrease in fluid spacing caused by PGG (Fig. 8), we postulate the existence of an additional attractive pressure. Previously we had argued that TA simultaneously binds to apposing bilayers, forming a molecular bridge between bilayers (Simon et al., 1994). Our data from compounds I–V provide the following support for this interpretation and indicate that compound V (PGG) also forms bridges between bilayers. First, the dipole potential, binding, and x-ray data indicate that PGG binds in the interfacial regions of the bilayers, changing the bilayer structure. Second, upon the addition of increasing concentrations of PGG only two equilibrium fluid spaces are observed, $d_f \approx 15$ Å for PGG concentrations of $<10^{-3}$ M and $d_f \approx 5$ Å for PGG concentrations of $>10^{-3}$ M (Fig. 8). This is consistent with a bridging mechanism, because membranes convert to the more stable state only when a sufficient number of bridges are formed to overcome the hydration, electrostatic, and steric pressures. Third, our experiments with compounds I–V indicate that to collapse the fluid space a molecule must contain between three and five gallic acids. A critical point in this argument for molecular bridging is that when the fluid spacing was decreased to 5

Å, the mole ratio of EPC:PGG was about 5:1. Because each PGG molecule contains five gallic acids (Fig. 1), this means that under conditions in which the fluid space was collapsed, each PC headgroup could potentially be in contact with a gallic acid residue. Thus the collapse of the fluid space occurs only when the entire surface is covered with polyphenols. Another factor that might be critical to the proposed bridging mechanism is the arrangement of gallic acids in PGG. Molecular models show that anhydrous PGG has a "globular" shape, with its five gallic acids projecting in different directions from the central D-glucose (Fig. 10). The molecular size of PGG ("diameter" $\approx$ 16 Å; see Fig. 10) and this distribution of gallic acids mean the PGG can span the interbilayer space and have gallic acids in contact with PC molecules from apposing bilayers. That is, because the width of each headgroup region of the bilayer is about 10 Å and the interbilayer space is about 5 Å for EPC-PGG (Fig. 8), it follows that gallic acid residues on opposite sides of PGG could simultaneously penetrate deep into the interfacial regions of apposing bilayers if the PGG spanned the interbilayer space. Even though compounds I, II, and III interact with PC and are sufficiently long to form bridges, because of their relatively low affinity (Table 1) and limited solubility, the surface concentrations of these polyphenols must remain below what is necessary to form a sufficient number of bridges. Compound IV, which has two gallic acids, also does not collapse the fluid spacing, most likely because the gallic acids in the 2 and 3 positions are on the same side of the glucose (Fig. 1) and thus one molecule cannot form bridges between membranes.

Tannic acid also caused the interbilayer fluid space to collapse to about 5 Å (Fig. 8). One similarity between PGG and TA is that they both have gallic acid or digallic residues extending in different directions from a central core. Our data suggest that PGG and TA collapse the fluid space at a concentration when each PC headgroup is in contact with one gallic or digallic acid. The similarity in the results shown in Fig. 8 indicate that the additional five gallic acids present on TA are not necessary to collapse the fluid spacing. However, because TA is a larger molecule than PGG, the observed similarity in fluid spacing implies that TA has to penetrate further into the bilayer interfacial region. In this regard, quadrupole splitting measurements revealed that TA perturbs the order of the first few methylene groups in the bilayer (Simon et al., 1994).

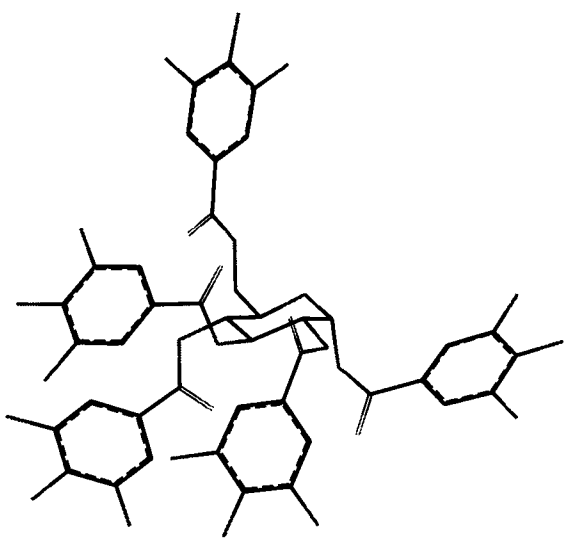

FIGURE 10 Figure of PGG constructed using Sybil program. The length of a gallic acid residue from its glucose linkage to its most distal OH group is about 6.5 Å, and the length of the central glucose molecule is about 3 Å. Therefore the length of PGG (in any of the five directions) is about 16 Å (= 6.5 Å + 6.5 Å + 3 Å).

At concentrations greater than 2.5×10^{-4} M, PGG binds to the membrane and increases the adhesion energy. Consequently, the total free energy of this interaction must be negative. Because at d_f = 5Å PGG must be conformationally restricted and hence have a reduced entropy of transfer, it follows that favorable enthalpic interactions between PGG and PC must occur. Indeed, with TA, the heat of binding to EPC was −8.3 kcal/mol (Simon et al., 1994). Such enthalpies should involve two types of attractive electrostatic interactions: an ion-dipole interaction between the electron rich π systems of the polyphenols and the $-N^+(CH_3)_3$ group on the lipids (Petti et al., 1988), and ion-ion interactions between the negatively charged polyphenol and the positively charged $-N^+(CH_3)_3$ moiety. In the latter case, to preserve electroneutrality, the Na^+ counterion would have to be associated with the phosphate moiety of PC. As long as the surface is not completely covered, the energy barrier arising from the repulsive hydration, undulation, and electrostatic pressures would be sufficiently large to keep the surfaces separated. In addition, the polyphenols in the fluid space may provide a steric barrier that prevents the surfaces from coming any closer. However, when all of the PC headgroups are associated with gallic acids the fluid space abruptly collapses (Fig. 8). The free energy driving this collapse is then enhanced by the attractive van der Waals interactions.

The involvement of the $-N^+(CH_3)_3$ groups of the PC molecules in the stabilization of the TA-PC complex is supported by the pioneering work of Kalina and Pease (1977), who noted that aqueous dispersions TA form a stable "complex" with DPPC. Kalina and Pease also reported (no data shown) that PGG and hexagalloylglucose are about as effective as TA in producing dispersions that are reactive to OsO_4. They did not, however, propose explanations based on physical principles of why these compounds reduced the periodic spacing in DPPC multilayers.

In summary, we have shown that selected polyphenols can induce PC bilayers to undergo a discontinuous transition in the fluid space. Although such discontinuous transitions have been observed with negatively charged lipids produced upon the addition of Ca^{2+} (Day et al., 1980; Cevc and Marsh, 1987; Rand and Parsegian, 1989), we believe that these polyphenols are the only small molecules known to collapse the fluid space upon binding to neutral bilayers.

This research was supported in part from National Institutes of Health grant GM27278 and a grant from the North Carolina Biotechnology Center.

REFERENCES

Andersen, S. O. 1970. Amino acid composition of spider silks. *Comp. Biochem. Physiol.* 35:705–711.

Armitage, R., G. S. Bayliss, J. W. Gramshow, E. Haslam, R. D. Haworth, K. Jones, H. J. Rogers, and T. Searle. 1961. Gallotannins. Part III. The constitution of Chinese, Turkish, sumach, and Tara tannins. *J. Chem. Soc.* 1842–1853.

Attard, P., D. J. Mitchell, and B. W. Ninham. 1988. The attractive forces between polar lipid bilayers. *Biophys. J.* 53:457–460.

Blaurock, A. E., and C. R. Worthington. 1966. Treatment of low angle x-ray data from planar and concentric multilayered structures. *Biophys. J.* 6:305–312.

Brockman, H. 1994. Dipole potential of lipid membranes. *Chem. Phys. Lipids.* 73:57–79.

Cevc, G., and D. Marsh. 1987. Phospholipid Bilayers: Physical Principles and Models. Wiley-Interscience, New York.

Chowdhy, B., Z., G. Lipka, and J. M. Sturtevant. 1984. Thermodynamics of phospholipid-sucrose interactions. *Biophys. J.* 46:419–422.

Damodaran, K. V., and K. M. Merz, Jr. 1994. A comparison of DMPC and DMPE-based lipid bilayers. *Biophys. J.* 66:1076–1087.

Day, E. P., Y. W. Kwok, S. K. Hark, J. T. Ho, W. J. Vail, J. Bentz, S. Nir, and D. Papahadjopolous. 1980. Reversibility of sodium-induced aggregration of sonicated phosphatidylcholine vesicles. *Proc. Natl. Acad. Sci. USA.* 77:4206–4029.

Evans, E. 1991. Entropy-driven tension in vesicle membranes and unbinding of adherent vesicles. *Langmuir.* 7:1900–1908.

Evans, E. 1994. Physical Actions in Biological Adhesion in Handbook of Physics of Biological Systems, Vol. 1. R. Lipowski, editor. Elsevier Science B. V. Netherlands. 697–727.

Evans, E., and D. Needham. 1988. Attraction between lipid membranes concentrated solutions of polymers: comparison of mean-field theory measurements of adhesion energies. *Macromolecules.* 21:1822–1831.

Evans, E. A., and V. A. Parsegian. 1986. Thermal-mechanical fluctuations enhance repulsion between bimolecular layers. *Proc. Natl. Acad. Sci. USA.* 83:7132–7136.

Guerette, P. A., D. G. Ginzinger, B. H. F. Weber, and J. M. Gosline. 1996. Silk properties determined by gland specific expression of spider fibron gene family. *Science.* 272:112–114.

Gustavson, K. H. 1956. The Chemistry of the Tanning Process. Academic Press, New York. 113–366.

Haslam, E. 1974. Polyphenol-protein interaction. *Biochem. J.* 139: 285–288.

Haslam, E., T. H. Lilly, Y. Cai, R. Martin, and D. Magnolato. 1989. Traditional herbal medicines: the role of polyphenols. *Planta Med.* 55:1–9.

Helfrich, W. 1973. Elastic properties of lipid bilayers: theory and possible experiments. *Z. Naturforsch.* 28C:693–703.

Helfrich, W., and R-M. Servuss. 1984. Undulations, steric interactions and cohesion of fluid membranes. *Il Nuovo Cimento.* 3:137–151.

Herbette, L., J. Marquardt, A. Scarpa, and J. K. Blasie. 1977. A direct analysis of lamellar x-ray diffraction from hydrated oriented multilayers of fully functional sarcoplasmic reticulum. *Biophys. J.* 20:245–272.

Hope, M. J., M. B. Bally, G. Webb, and P. R. Cullis. 1985. Production of large unilamellar vesicles by rapid extrusion procedure: characterization of size distribution, trapped volume, and ability to maintain a membrane potential. *Biochim. Biophys. Acta.* 812:55–65.

Hunter, R. J. 1986. Foundations of Colloid Science. Oxford University Press, Oxford.

Israelachvili, J. N. 1985. Book Intermolecular and Surface Forces. Academic Press, London.

Israelachvili, J. N., and H. Wennerstrom. 1990. Hydration or steric forces between amphiphilic surfaces? *Langmuir.* 6:873–876.

Israelachvili, J. N., and H. Wennerstrom. 1992. Entropic forces between amphiphilic surfaces in liquids. *J. Phys. Chem.* 96:520–531.

Kalina, M., and D. C. Pease. 1977. The preservation of ultrastructure in saturated phosphatidylcholines by tannic acid in model systems and type II pneumocytes. *J. Cell. Biol.* 74:726–741.

Kaminoh, Y., C. Tashiro, H. Kamaya, and I. Ueda. 1988. Depression of phase-transition temperature by anesthetics: nonzero solid binding. *Biochim. Biophys. Acta.* 946:215–220.

LeNeveu, D., R. P. Rand, V. A. Parsegian, and D. Gingell. 1977. Measurement and modification of forces between lecithin bilayers. *Biophys. J.* 18:209–230.

Lesslauer, W., J. E. Cain, and J. K. Blasie. 1972. X-ray diffraction studies of lecithin bimolecular leaflets with incorporated fluorescent probes. *Proc. Natl. Acad. Sci. USA.* 69:1499–1503.

Lipowski, R. 1994. Discontinuous unbinding transitions of flexible membranes. *J. Phys. (Paris).* 4:1755–1762.

MacDonald, R. C., and S. A. Simon. 1987. Lipid monolayer states and their relationship to bilayers. *Proc. Natl. Acad. Sci. USA.* 84:4089–4094.

Marcelja, S., and N. Radic. 1976. Repulsion of interfaces due to boundary water. *Chem. Phys. Lett.* 42:129–130.

Marrink, S-J., M. Berkowitz, and H. C. Berendsen. 1993. Molecular dynamics simulations of a membrane/water interface: the ordering of water and its relation to the hydration force. *Langmuir.* 9:3122–3131.

McDaniel, R. V., T. J. McIntosh, and S. A. Simon. 1983. Non-electrolyte substitution for water in lecithin bilayers. *Biochim. Biophys. Acta.* 731: 97–108.

McIntosh, T. J. 1980. Differences in hydrocarbon chain tilt between hydrated phosphatidylethanolamine and phosphatidylcholine bilayers: a molecular packing model. *Biophys. J.* 29:237–246.

McIntosh, T. J., S. Advani, R. E. Burton, D. V. Zhelev, D. Needham, and S. A. Simon. 1995. Experimental tests for protrusion and undulation pressures in phospholipid bilayers. *Biochemistry.* 34:8520–8532.

McIntosh, T. J., A. D. Magid, and S. A. Simon. 1987. Steric repulsion between phosphatidylcholine bilayers. *Biochemistry.* 26:7325–7332.

McIntosh, T. J., A. D. Magid, and S. A. Simon. 1989a. Cholesterol modifies the short-range repulsive interactions between phosphatidylcholine membranes. *Biochemistry.* 28:17–25.

McIntosh, T. J., A. D. Magid, and S. A. Simon. 1989b. Range of the solvation pressure between lipid membranes: dependence on the packing density of solvent molecules. *Biochemistry.* 28:7904–7912.

McIntosh, T. J., A. D. Magid, and S. A. Simon. 1989c. Repulsive interactions between uncharged bilayers. Hydration and fluctuation pressures for monoglycerides. *Biophys. J.* 55:897–904.

McIntosh, T. J., R. V. McDaniel, and S. A. Simon. 1983. Induction of an interdigitated gel phase in fully hydrated lecithin bilayers. *Biochim. Biophys. Acta.* 731:109–114.

McIntosh, T. J., and S. A. Simon. 1986a. Area per molecule and distribution of water in fully hydrated dilauroylphosphatidylethanolamine bilayers. *Biochemistry.* 25:4948–4952.

McIntosh, T. J., and S. A. Simon. 1986b. The hydration force and bilayer deformation: a reevaluation. *Biochemistry.* 25:4058–4066.

McIntosh, T. J., and S. A. Simon. 1993. Contribution of hydration and steric (entropic) pressures to the interaction between phosphatidylcholine bilayers: experiments with the subgel phase. *Biochemistry.* 32: 8374–8384.

McIntosh, T. J., and S. A. Simon. 1994a. Hydration and steric pressures between phospholipid bilayers. *Annu. Rev. Biophys. Biomol. Struct.* 23:27–51.

McIntosh, T. J., and S. A. Simon. 1994b. Long- and short-range interactions between phospholipid/ganglioside GM1 bilayers. *Biochemistry.* 33:10477–10486.

McIntosh, T. J., and S. A. Simon. 1996. Adhesion between phosphatidylethanolamine bilayers. *Langmuir.* 12:1622–1630.

McIntosh, T. J., S. A. Simon, J. C. Ellington, Jr., and N. A. Porter. 1984. A new structural model for mixed-chain phosphatidylcholine bilayers. *Biochemistry.* 23:4038–4044.

Nash, T., A. C. Allison, and J. S. Harington. 1966. Physio-chemical properties of silica in relation to toxicity. *Nature.* 210:259–261.

Nowick, J. S., T. Cao, and G. Noronha. 1994. Molecular recognition between uncharged molecules in aqueous micelles. *J. Am. Chem. Soc.* 116:3285–3289.

Oh, H. I., J. E. Hoff, G. S. Armstrong, and L. A. Haff. 1980. Hydrophobic interaction in tannin:protein complexes. *J. Agric. Food Chem.* 28: 394–398.

Parsegian, V. A., N. Fuller, and R. P. Rand. 1979. Measured work of deformation and repulsion of lecithin bilayers. *Proc. Natl. Acad. Sci. USA.* 76:2750–2754.

Parsegian, V. A., R. P. Rand, P. Fuller, and D. C. Rau. 1986. Osmotic stress for the direct measurement of intermolecular forces. *Methods Enzymol.* 127:400–416.

Petti, M. A., T. J. Shepodd, R. E. Barrans, Jr., and D. A. Dougherty. 1988. "Hydrophobic" binding of water soluble guests by high-symmetry, chiral hosts. An electron-rich receptor site with a general affinity for quaternary ammonium compounds and electron-deficient 213 systems. *J. Am. Chem. Soc.* 110:6825–6840.

Ranck, J. L., T. Keira, and V. Luzzati. 1977. A novel packing of the hydrocarbon chains in lipids. The low temperature phase of DPPG. *Biochim. Biophys. Acta.* 488:432–441.

Rand, R. P., N. Fuller, V. A. Parsegian, and D. C. Rau. 1988. Variation in hydration forces between neutral phospholipid bilayers: evidence for hydration attraction. *Biochemistry.* 27:7711–7722.

Rand, R. P., and V. A. Parsegian. 1989. Hydration forces between phospholipid bilayers. *Biochim. Biophys. Acta.* 988:351–376.

Reyes, J., F. Greco, R. Motais, and R. Latorre. 1983. Phloretin and phloretin analogues: mode of action. *J. Membr. Biol.* 72:93–103.

Rudolph, A. S., and B. Goins. 1991. The effect of hydration stress on the phase behavior of hydrated dipalmitolyphosphatidylcholine. *Biochim. Biophys. Acta.* 1066:90–94.

Schrijvers, A. H. G. J., P. M. Frederik, M. C. A. Stuart, K. N. J. Burger, and R. S. Reneman. 1989. Formation of multilamellar vesicles by addition of tannic acid to phosphatidylcholine-containing small unilamellar vesicles. *J. Histochem. Cytochem.* 37:1653–1643.

Seddon, J. M., G. Cevc, R. D. Kaye, and D. Marsh. 1984. X-ray diffraction study of the polymorphism of hydrated diacyl- and dialkylphosphatidylethanolamines. *Biochemistry.* 23:2634–2644.

Shan, S-ou, S. Loh, and D. Herschlag. 1996. The energetics of hydrogen bonds in model systems: implications for enzymatic catalysis. *Science.* 272:97–101.

Simon, S. A., S. Advani, and T. J. McIntosh. 1995. Temperature dependence of the repulsive pressure between phosphatidylcholine bilayers. *Biophys. J.* 69:1473–1483.

Simon, S. A., E. A. Disalvo, K. Gawrisch, V. Borovyagin, E. Toone, S. S. Schiffman, D. Needham, and T. J. McIntosh. 1994. Increased adhesion between neutral lipid bilayers: interbilayer bridges formed by tannic acid. *Biophys. J.* 66:1943–1958.

Simon, S. A., C. A. Fink, A. K. Kenworthy, and T. J. McIntosh. 1991. The Hydration pressure between lipid bilayers: a comparison of measurements using x-ray diffraction and calorimetry. *Biophys. J.* 59:538–546.

Simon, S. A., and T. J. McIntosh. 1984. Interdigitated hydrocarbon chain packing causes the biphasic transition behavior in lipid/alcohol suspensions. *Biochim. Biophys. Acta.* 773:169–172.

Simon, S. A., and T. J. McIntosh. 1989. Magnitude of the solvation pressure depends on dipole potential. *Proc. Natl. Acad. Sci. USA.* 86: 9263–9267.

Simon, S. A., T. J. McIntosh, and A. D. Magid. 1988. Magnitude and range of the hydration pressure between lecithin bilayers as a function of head group density. *J. Colloid Interface Sci.* 126:74–83.

Simon, S. A., T. J. McIntosh, A. D. Magid, and D. Needham. 1992. Modulation of the interbilayer hydration pressure by the addition of dipoles at the hydrocarbon/water interface. *Biophys. J.* 61:786–799.

Smejek, P., and S. Wang. 1990. Adsorption to dipalmitoylphosphatidylcholine membranes in gel and fluid state: pentachlorophenolate, dipicrylamine and tetraphenylborate. *Biophys. J.* 58:1285–1294.

Springer, T. A. 1990. Adhesion receptors in the immune system. *Nature.* 346:425–434.

Swarmy, M. J., and D. Marsh. 1995. Thermodynamics of interdigitated phases of phosphatidylcholine in glycerol. *Biophys. J.* 69:1402–1408.

Tardieu, A., V. Luzzati, and F. C. Reman. 1973. Structure and polymorphism of the hydrocarbon chains of lipids: a study of lecithin-water phases. *J. Mol. Biol.* 75:711–733.

Tatulain, S. A. 1983. Effect of lipid phase transition on the binding of anions to dimyristoylphosphatidylcholine liposomes. *Biochim. Biophys. Acta.* 736:189–195.

Waite, J. H. 1983. Evidence for a repeating 3,4-dihydroxyphenylalanine- and hydroxyproline-containing decapeptide in the adhesive protein of the mussel, *Mytilus edulis* L. *J. Biol. Chem.* 258:2911–2933.

Weast, R. C. 1984. Handbook of Chemistry and Physics. CRC Press, Boca Raton, FL. E-42.

Zhang, C., and G. Vanderkooi. 1992. Molecular origin of internal dipole potential in lipid bilayers: calculation of the electrostatic potential. *Biophys. J.* 69:935–941.